The current status of mangrove forests in Spanish Lagoon (Aruba) evaluated from a hydrological point of view

Assessing the water balance and modelling tree growth rates

Proposal by: Siebe Houtsma
Supervisors: Klaas Metselaar (WUR)
Emil ter Horst
Tatiana Becker

I Abstract

The importance of mangroves is widely recognized because of the number of services they provide (e.g. habitat function and coastal protection). In this study the current status of the mangrove forest in Spanish Lagoon (Aruba) is evaluated from a hydrological point of view, in order to determine whether these services are threatened. During a three month period of fieldwork both the salt and freshwater supply was quantified. In addition, the biomass of the forest was estimated. The average biomass found in this study compares reasonably well to those found in Puerto Rico and Sri Lanka.

Moreover, a model was developed to simulate tree growth under the current hydrological regime. Mangrove growth in the canal, which is in open connection with the sea, was compared to growth in the hinterland of Spanish Lagoon. The model results indicate that growth is not limited in the current hydrological conditions, neither for the mangroves along the canal nor for the mangroves in hinterland. However, a sensitivity analysis shows that the hinterland is sensitive to increased salt concentrations. Blocking of seawater inflow by mangroves is the biggest threat for tree growth in the hinterland, since it can lead to increased salt concentrations; potentially causing a reduced tree growth.

Table of Contents

1. Introduction

Mangroves are woody plants that predominantly grow in tropical and subtropical climates at the transition from land to sea. In total the mangrove family consists of 69 different species of which most can be found in the Indo West Pacific (Duke, 1992). Being exposed to tidal flooding, mangroves have to cope with varying salt concentrations. Different mechanisms, including salt-excreting leaves or ultra-filtration at the root cell membranes, enable water uptake by mangrove trees under saline conditions (Parida & Jha, 2010). However, the extent to which mangroves survive saline conditions differs per species (Ball, 1988); some species can withstand high salt concentrations up to 75% seawater, whereas growth of other species is already reduced at low concentrations due to stress (Downton, 1982; Clough, 1984). These differences in tolerances lead to a clear zonation in mangrove forests.

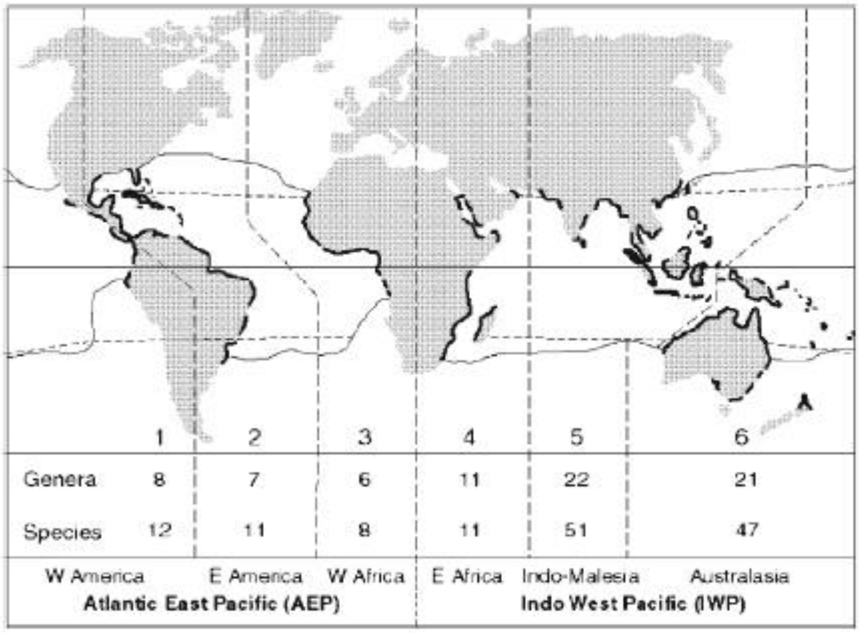

Figure 1 – Global distribution of mangroves (Alongi, 2009)

Globally, the total area covered by mangroves declined considerably over the past decades. Research by the FAO (2003) indicated losses of approximately 2% on yearly basis between 1980 and 1990, and approximately 1% between 1990 and 2000. The main causes for this decline are urbanization, aquaculture, mining and overexploitation for timber, fish, crustaceans, and shellfish (Alongi, 2008). Given the fact that coastal ecosystems such as mangroves offer a number of important services – for example the habitat function for numerous species, coastal protection, and retention of carbon and nutrients (Nagelkerken et al., 2008; Danielsen et al, 2005; Lovelock & Ellison, 2007) – conservation of these type of ecosystems is necessary for maintaining biodiversity and protection against flooding and erosion (FAO,1994). The importance of these services has also been recognized by the Ramsar Convention, which defines "conservation and wise use of wetlands" as its mission (Ramsar, 2016a).

1.1 Problem description

Spanish Lagoon, described by Ramsar (2016a) as "a narrow coastal inlet fringed by tidal mudflats and mangrove swamps", is Aruba's only site that is part of this convention. To date little research has been done on this specific Ramsar site with respect to mangrove growth, although the quality of the forest has to meet the guidelines defined by the convention (Ramsar, 2016b). Therefore, there is a need to quantify the hydrological processes and determinants that affect the quality of mangroves in order to assess to what extent the function as a breeding place for bird and fish of this specific Ramsar site is in danger.

This study is aimed at analysing and evaluating the current status of the mangrove forest in order to maintain the services provided by this ecosystem. The data that is necessary for this analysis was gathered during fieldwork over a period of around three months. Based on these data tree growth in Spanish Lagoon can be related to the hydrology. By quantifying the different terms of the water balance valuable information of the current status of the mangrove forest can be obtained, because growth and composition of the forests are affected by evaporation and freshwater supply (Jimenez, 1992). Several other studies also indicate the importance of water quantity as well as quality for mangrove growth (Twilley & Chen, 1998; Kraus et al., 2007; Calderon et al., 2014). Moreover, according to Gondwe et al. (2010) understanding of the hydrology is required to manage the water resources of mangrove ecosystems.

Another aspect of this study is to model mangrove growth in order to evaluate the quality of the forest in terms of biomass and the vulnerability to changing hydrological conditions. According to Erwin (2009) changes in hydrological regimes due to climate change have drastic implications for vulnerable wetland ecosystems such as mangroves and moreover will impede restoration projects. The model developed for this evaluation simulates tree growth in terms of above-ground biomass production. A comparison will be made between biomass production of mangroves growing in open water and mangroves growing in the hinterland to investigate whether local differences in hydrological fluxes affect the biomass production.

This report describes exploratory research and provides a basis for additional research at Aruba on for example erosion, restoration or climate change.

1.2 Research questions and objectives

Considering the lack of (mainly) hydrological data and the implications of both the current and future hydrological regime on mangrove tree growth the following questions were formulated:

- *What is the current status of mangrove forest at Aruba from a hydrological perspective?*
    - What is the level of moisture stress?
    - What is the level of salt stress?

- *What is the quality of the mangrove trees in terms of biomass?*
    - What is the current average biomass of the trees? And how does this compare to the biomass found for mangroves forests in other regions?
    - What is the long-term biomass production under the current hydrological conditions?

2. Study area

The study area, Spanish Lagoon (12º30'N 070º00'W), is located on the southwestern side of Aruba along the coast; around 10 kilometres southeast of Oranjestad (figure 2). The surface area covers around 70 hectares and the length of the tidal inlet is approximately 2 kilometres (DCNA, 2016). The inlet is fringed by tidal mudflats and mangrove swamps (Ramsar, 2016a). Within this site four different mangrove species can be distinguished, which are *Rhizophora mangle*, *Avicennia germinans*, *Laguncularia racemosa*, *Conocarpus erecta*. Along the canal predominantly red mangroves (*R. mangle*) can be found, whereas black mangroves (*A. germinans*) dominate in the forest in the hinterland of the area. The other species occur at the drier parts of the area and are less frequently observed.

The study site is split up in two parts in order to compare biomass production in open water to production in the hinterland. Hereafter, the part from the edge of the forest towards the sea will be referred to as "tail" (the area indicated by the red line). The part of study site where the mangrove forest starts (at the end of the canal) towards the road further landward will be referred to as "head" (the area indicated by the green line). To get a better impression, please consult figure 1 in the annex.

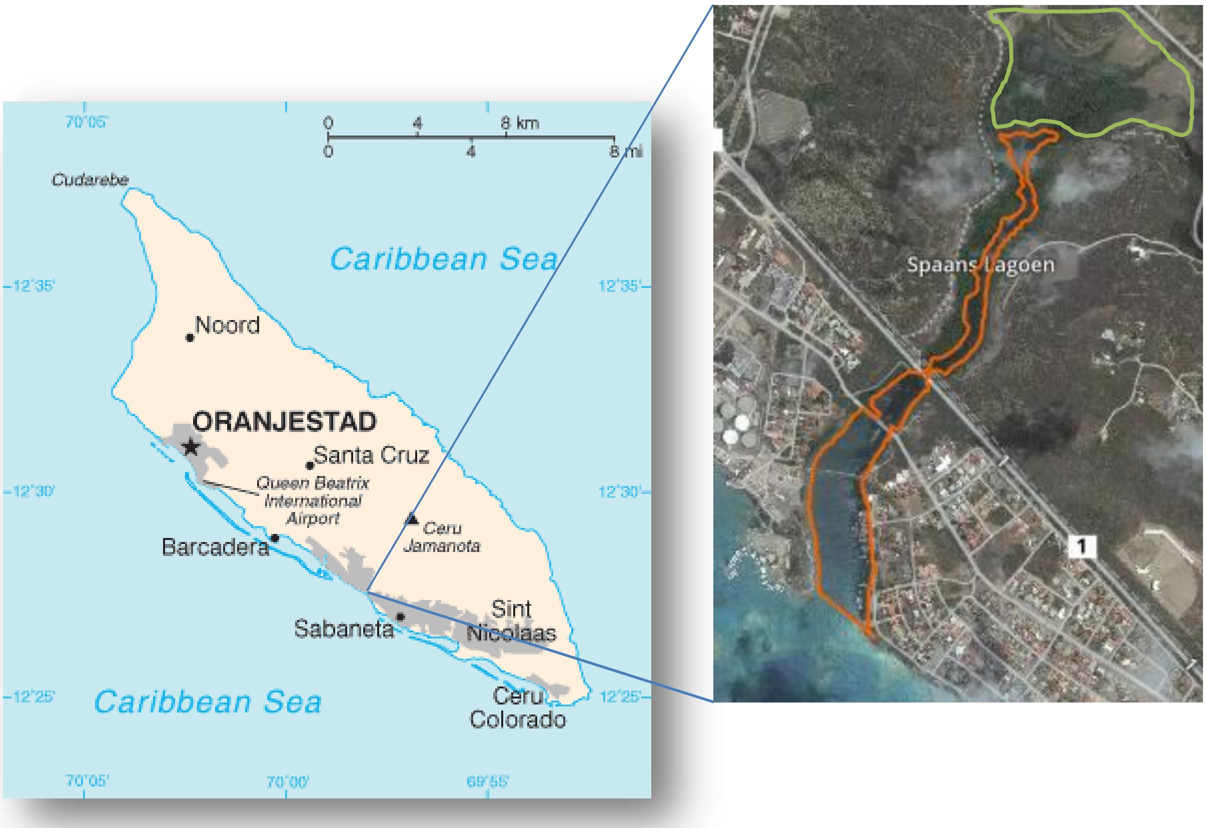

Figure 2 – Map of Aruba (left panel) and of the study area, Spanish Lagoon (right panel)

2.1 Catchment area

The catchment area of Spanish Lagoon is determined using a digital elevation model (DEM). A hydro-tool in ArcGIS was used in order to divide the catchment into subcatchments. Given the large size of the catchment (15.1 km^2), which is too extensive to analyse completely, only the subcatchments that are directly connected to Spanish Lagoon are taken into account. Such an analysis would also go beyond the scope of this study. Moreover, mangroves only occur in the selected area of the catchment (2.6 km^2). Figure 3 gives an overview of the catchment and the selected subcatchments.

Figure 3 – Overview of the catchment area of Spanish Lagoon; the dark green area is the entire catchment and the light green area the selected part of the catchment for this study.

2.2 Climate

According to the Köppen Climate Classification System Aruba has a tropical steppe, semi-arid hot climate. There is a dry season running from February to June and a rainy season from September to January. The annual of amount of rainfall was 471.7 mm for the period 1981-2010. The average temperature in this period was 28.1 °C, ranging from 26.7 °C in the coolest months to 29.2 °C in the warmest months. The wind predominantly blows from the eastern direction with an average speed at 10 meter height of 7.3 m/s (Departemento Meteorologico Aruba, 2016).

2.3 (Hydro)geology

Aruba is situated at the boundary of the Caribbean and South-American plates. The strongly folded successions of volcanics and sediments, which form the basis of this island, indicate movement of these plates during the Cretaceous and Early Tertiary (Van Sambeek et al., 2000). The igneous rocks that occur at Aruba, which also occur at Bonaire and Curacao, indicate that the islands were formed by a chain of volcanoes above the subducting plate; these chains are also known as volcanic arcs. Collision with the South-American continent in the Early Tertiary caused uplift of the continental margin resulting in folding, faulting and metamorphism of the rocks at Aruba (Van Sambeek et al., 2000). However, large parts of the older rocks are removed by erosion.

In addition to the igneous rocks, limestone terraces occur as small patches over the coastal region. So limestone formation forms the geological basis of the study area. These limestone terraces were formed as a result of changing sea levels during the Quartenary in combination with slow tectonic uplift (Van Sambeek et al., 2000). Along the southwestern coast of Aruba erosional terraces are found. In contrast to the windward side the coast on this side of the island is not steep. Here, a ridge made up of coral shingle, beach rock and sandy deposits is located. Coral reef is found in front of this ridge (Grontmij & Sogreah, 1968).

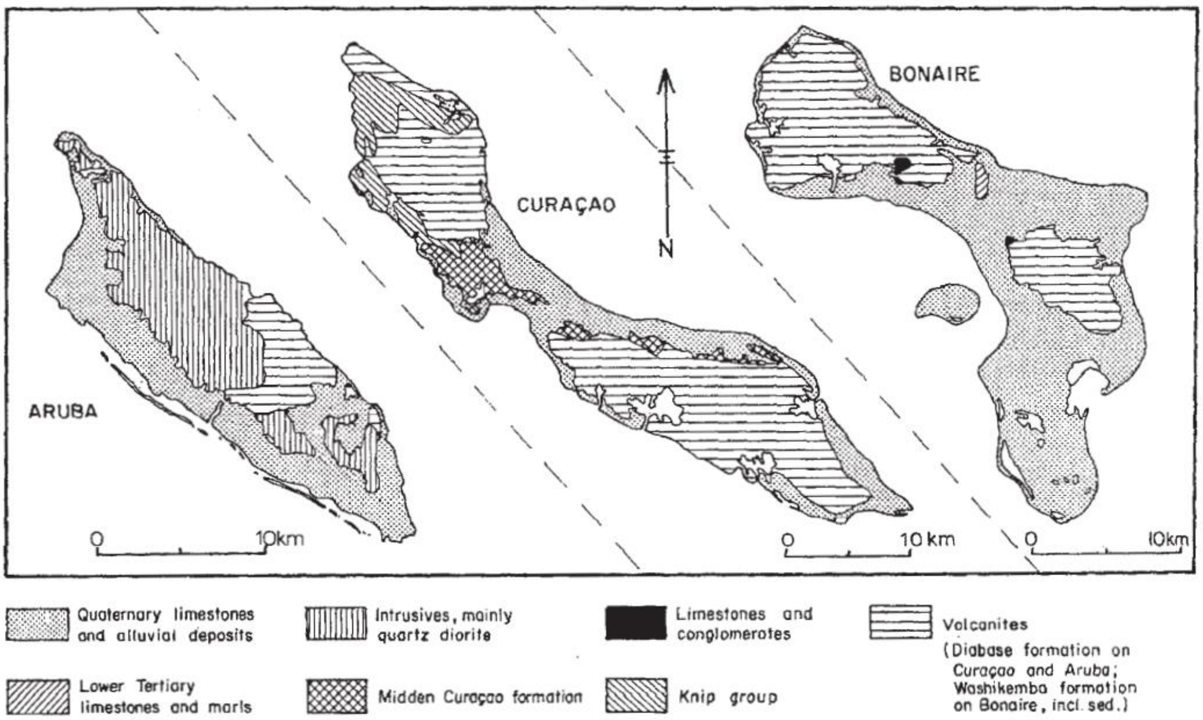

Figure 4 – Geological map of Aruba, Curacao and Bonaire (Van Sambeek et al., 2000)

Groundwater flow through limestone, coral reef and karst is rather complex (Van Dam et al., 2015). This since limestones can be very permeable because of karstic phenomena, which is the case on Aruba (Van Sambeek et al., 2000). Also the coral limestones have a rather high permeability as a result of the great number of cracks and jointings. In a study to coral-reef hydrology Oberdorfer & Buddemeier (1986) found that the hydraulic conductivity of reef plates ranged from 0.8 to 2.8 m/d. At some parts of Aruba crystalline rock or alternating sand-clay layers underlie the limestone. Groundwater flow in crystalline rock occurs through fractures or the (shallow) weathered zones (Grontmij & Sogreah, 1968). Small aquifers in the sand and clay layers might be saturated with seawater (De Buisonjé, 1974). A simplified map of the geology of Aruba is given in figure 4.

3. Methodology and approach

3.1 Fieldwork

3.1.1 Rainfall and rainfall interception

Rainfall was measured using a tipping bucket rain gauge. The gauge was installed at the leeward side of the vegetation to minimize the effect of the wind on the measurements. A plank was used to level the gauge on the rocky subsoil. The gauge was connected to a datalogger that registered the amount of rainfall every five minutes.

Twenty PET bottles (see figure 5) were installed at five different locations distributed over the study area. So at each plot four bottles were placed; three beneath the canopy and one next to the canopy. The latter represented an ordinary rain gauge, whereas the other gauges were used to measure the amount of troughfall.

Figure 5 – Example of a PET bottle used for estimating the rainfall interception. This specific bottle represents an ordinary rain gauge, throughfall gauges were installed below the canopy.

For this experiment 20 identical 1,5L PET bottles were used. The diameter of the bottles was 8.5 cm and the heights were approximately 28 cm. As showers occurred quite often during night time, the amount of water collected by the bottles was measured the next morning. The collected water was poured from the PET-bottles into a measuring cup; a sieve was used to remove litter and insects from the water. In addition the amount of water was weighed and then converted to mm. The difference in the amount of water collected by the rain gauge and the throughfall gauges is a measure of the interception. Given the fact that during night time evaporation is minimal, it was assumed that the effect of evaporation can be neglected.

3.1.2 Evaporation

The pan used for measuring the evaporation was an aluminium cooking pan. The diameter of the pan was 38.0 cm and the height 22.5 cm. On both sides of the pan a handle was attached. These handles exceed the edge of the pan by approximately 5 cm. To prevent animals from drinking out of the pan, the pan was covered with gauze; the gauze had a mesh size of 2.5 x 2.5 cm. See figure 6 for the measurement setup.

Figure 6 – Measurement setup for precipitation and evaporation.

A pressure sensor (Honeywell ABPDJJ001PGAA5) registered the water height in the pan every five minutes. The pressure sensor was connected to the same datalogger as the automatic rain gauge. Once every two to four days the water level in the pan was measured manually. In case the water level dropped to a level around 5 cm above the sensor the pan was refilled.

The pan was put and leveled on a spot where it was exposed to sunlight for nearly the whole day. The vegetation in the vicinity of the pan consisted of bushes that reached heights of 1.5 m at maximum. So, given both the angle of the sun and the distance of these bushes from the pan, the impact of shading is assumed to be minor. The presence of bushes might have lead to a reduction of the wind speed and consequently to a reduction of the evaporation.

3.1.3 Seawater inflow

Five divers were installed in a transect to measure the effect of tides at multiple locations in Spanish Lagoon. Four divers were located in the canal and one behind the forest in the hinterland. The distance between the measurement points was around 400-600 m. The pressure of the water column above the diver was measured every 15 minutes.

Salinity
The salinity of seawater was measured using an electrical conductivity (EC)meter. Thirteen samples were collected in a transect, starting at the inlet and ending in the hinterland. Since the values exceeded the measuring range of the device the samples had to be diluted with tap water (EC: 0.04 mS/cm). This dilution process was done with use of a measuring cup.

3.1.4 Soil properties

Hydraulic functions
Several soil (hydraulic) properties were measured including the hydraulic conductivity. This was done using a minidisc portable tension infiltrometer (Decagon Devices, Pullman, WA). Two different versions of the minidisc infiltrometer (MDI) exist. In this study a MDI with a bubbling chamber was used (version 2). The conductivity was determined at two locations along the head of Spanish Lagoon. The measurements were repeated once in order to get insight in the temporal variation.

For determining the soil texture soil samples were taken at 10 different locations along the inlet. The soil samples were put in glass jars and subsequently filled with water (FAO Training Series, 2017). First the mixture had to be stirred, so all particles were in suspension. Then let the mixtures settle and from the proportions sand, silt and clay the soil texture could be determined. Furthermore, soil samples were taken at four different locations along the head using soil rings. At the locations the water had just retreated and therefore the soils were still saturated. The samples were weighed before and after drying, so the volumetric water content could be determined.

Finally, the depth of the sediment layer in the hinterland was determined. Two divers were installed in PVC tubes at different depths; one at circa 1 m depth and the second at circa 2 m depth. These divers registered the pressure head at both depths. The difference in the pressure heads give an indication of thickness of the sediment layer.

Salinity
Soil samples along two different transects were taken. The first transect consisted of four points along the “head” of Spanish Lagoon, the second consisted of six points along the tail. After a few weeks of drying the samples were sieved and subsequently the saturated paste method was applied.

For measuring the salinity of the soil an adapted version of the saturated paste extraction method was used. The bottle neck of a PET bottle was cut off and put upside down in the bottom part. In the funnel-shaped bottle neck a coffee filter was placed. This filter was then filled with the saturated soil. These samples were prepared using the saturated paste method described by Rhoades and Chanduvi (1999). By rotating the bottle at high speed the water ran through the filter and ended up in the bottom part of the bottle. The electrical conductivity of the filtered water could then be measured. In case the salinity exceeded the measuring capacity of the EC meter, the water had to be diluted with tap water.

The amount of salts in the soil profile in kg/m^2 could be determined using the equation described in a study by Van Hoorn and Van Alphen (1994), which is as following:

$$\boldsymbol{S = C * w * D * \frac{\rho_b}{\rho_w}} \qquad (1)$$

3.1.5 Tree growth

To monitor tree growth four plots were installed distributed over the study area. At each plot six trees were selected and marked with a yellow ribbon (see figure 7). The ribbon was tied to the tree

Figure 7 – One of the biomass monitoring plots. The yellow ribbon indicates the position where the perimeter was measured.

at breast height (1.3 m above soil surface). Once a month the perimeter of the tree at this height was measured with a flexible measuring tape. The perimeter of the tree needs to be converted to diameter in order to calculate the biomass of the tree. Imbert and Rollet (1989) present an equation for estimating the above-ground biomass (W_{top} in kg) of *R. mangle* based on DBH measurements.

$$\boldsymbol{W_{top} = 0.178 * DBH^{2.47}} \quad (2)$$

In addition, fisheye pictures were taken with a fisheye lens (TAO tronics, model: TT-SH014) that is specifically designed for smartphone cameras. From these pictures the leaf area index (LAI) could be estimated. Height of the trees were measured using an Android application for smartphones called "measure height". A copper tube was used to measure the depth of the soil in order to get insight the extent of the rooting depth.

The program Gap Light Analyzer (Frazer et al., 1999), referred to as GLA, was used to estimate the LAI. This program uses hemispherical photographs of the canopy as input and converts these pictures to black-white images. These photographs have to be taken with a hemisperical lens with a full 180° field of view and known projection distortion. By changing the brightness of the pictures a distinction between the sky and leaf fraction is made; where white represents the part of the image that is sky and black the part that is leaves. This fraction is calculated based on a zenith angle from 0° to 60° (Stenberg et al., 1994). For the best estimates pictures should be taken under conditions of uniform cloud cover.

Finally, the crop coefficient (k_c) of *R. mangle* could be calculated using the LAI and the extinction coefficient of this crop and those of a reference crop (Van Dam et al., 2015). The ratio of the potential evapotranspiration and the reference potential evapotranspiration is the crop coefficient, in case the soil evaporation is assumed to be zero.

3.2 Water and salt balance

For the evaluation of the growth conditions of mangrove trees during the fieldwork period both the water balance and the salt balance were set up. Growth reduction – from a hydrological point of view – occurs as a results of either water stress or salt stress. Hence, two stress parameters defined by Van Dam et al. (2015) were used to calculate the extent to which growth was limited. Water stress was calculated with equations 3 and salt stress with equation 4. Both equations provide a value between 0 and 1; values <1 indicate growth limitation caused by stress. The combination of both parameters is a measure for the growth performance.

$$\boldsymbol{\omega_w = \left(\frac{W}{W_x}\right)^b} \tag{3}$$

where W and W_x are the storage and maximum storage in mm and b the parameter that indicates how the reduction in transpiration changes between field capacity and wilting point. For this study b was set to 1, so the reduction is assumed to be linear.

$$\boldsymbol{\omega_s = \begin{cases} \left(1 - \frac{EC - EC_{max}}{EC_{max}}\right) \; if \; 0 < \left(1 - \frac{EC - EC_{max}}{EC_{max}}\right) < 1 \\ 0 \quad if \; \left(1 - \frac{EC - EC_{max}}{EC_{max}}\right) < 0 \end{cases}} \tag{4}$$

where EC and EC_{max} are the electrical conductivity and the maximum electrical conductivity in mS/cm respectively. According to Chen and Twilley (1998) the salt tolerance of *R. mangle* is 70 g/kg seawater. Considering the density of seawater, which is approximately 1 kg/l, the salinity can also be expressed in g/l. Next the salt concentration can be converted to the electrical conductivity by dividing the concentration by 0.7, resulting in an EC of 100 mS/cm (Van Hoorn and Van Alphen, 1994).

3.2.1 Setting up the water balance

Hydrology in coastal ecosystems
Hydrology in mangrove ecosystems, or more generally, coastal ecosystems differs from ordinary hydrology which only involves freshwater. Due to tides in coastal ecosystems salt water enters these systems and mixes with freshwater. The salinity in such an environment is, however, not solely regulated by tides, but also channels and the associated hydraulics play an important role in this (Van Dam et al., 2015). Blocking of channels as a result of growth can lead to changes in the salt balance of total system.

The seawater inflow in this study was obtained from the diver data. From the differences between high and low tide the daily seawater influx could be derived which was calculated by subtracting the water level during low tide from the water level during high tide. In case of multiple tidal currents occurred on one day, the values were added together. Since the signal of the divers contained noise the signal had to be smoothed first in order to remove local minima and maxima. These local minima and maxima could incorrectly contribute to the total influx and therefore lead to an overestimation. The procedure of smoothing the signal was done using the fast Fourier transform method.

The total water balance

As described in the previous section, the majority of the terms needed to set up the water balance were measured during fieldwork. For runon and drainage, however, this is not the case. Runon from the upstream part of the catchment that flows into the selected area was calculated under the conservative assumption that it was a fixed fraction of the amount of precipitation. In a study to water resources of the Netherlands Antillles Grontmij & Sogreah (1968) found that values for surface runoff ranged from 10-14% of the total amount of rainfall. Since the slopes in the downstream part of the study site in general were rather gentle, the runon is assumed to be 10% of the total amount of rainfall. In fact, the concentration factor should also be taken into account. This factor corrects for the difference in size of the upstream area and the downstream area. However, Bracken and Croke (2007) discuss the concept of hydrological connectivity and indicate that not all water that is potentially available for runoff will actually end up in the downstream area. This, to some extent, compensates for ignoring the concentration factor and hence this assumption is justifiable.

So, now the change in storage (ΔW) on daily basis can be calculated using the following equation:

$$\Delta \boldsymbol{W} = \boldsymbol{P} - \boldsymbol{I} - \boldsymbol{ET} + \boldsymbol{F_R} + \boldsymbol{F_{in}} - \boldsymbol{D} \quad \textbf{(5)}$$

In the equation above P represents rainfall, I rainfall interception, ET evapotranspiration, F_R runon, F_{in} seawater influx and D drainage; all quantities are in mm. The total storage is dependent on the soil depth and the available water content (AWC), which differs per soil type. In this study the soil was assumed to consist of silty to clayey material. The AWC of clay is 0.15 (USDA, 2017) and the depth of the sediment layer was estimated on 2 m. So, the total storage per m^2 is 300 mm. Water that cannot be stored in the soil anymore will be drained. As already mentioned in the introduction, a distinction is made between mangroves along the canal and in the hinterland. So, for both locations the water balance is set up.

3.2.2 Coupling to the salt balance

In order to determine whether growth conditions for mangroves are under pressure due to for example salinity stress, the water balance is coupled to the salt balance. The salt balance is linked to the water balance via the soil storage, since the storage indicates how much water can enter the soil. Changes in the total amount of salt ΔS can be described by the equation below, where F_{in} and F_{out} represent the incoming and outgoing water flux in mm respectively, c_0 the salt concentration of the incoming water in g/l and c the salt concentration after mixing. The incoming flux has a salinity close to that of seawater, so for c_0 the salt concentration of seawater is used.

$$\Delta \boldsymbol{S} = \boldsymbol{F_{in}} \boldsymbol{c_0} - \boldsymbol{F_{out}} \boldsymbol{c} \quad \textbf{(6)}$$

The concentration per square meter for a given soil depth can also be written as $c = \frac{S}{W}$ and the outgoing flux as $F_{out} = D$, resulting in the following equation:

$$\Delta \boldsymbol{S} = \boldsymbol{F_{in}} \boldsymbol{c_0} - \boldsymbol{D} \frac{\boldsymbol{S}}{\boldsymbol{W}} \quad \textbf{(7)}$$

The total salt content (S_t) in the soil for a given time step can be calculated by adding the change in concentration to the concentration of the previous time step (equation 8). In this study daily changes in salt concentrations are calculated.

$$\boldsymbol{S_t} = \boldsymbol{S_{t-1}} + \Delta \boldsymbol{S} \Delta \boldsymbol{t} \quad \textbf{(8)}$$

3.3 Model setup

3.3.1 Model description and data

The model used for simulating long-term tree growth is relatively simple. A tree growth equation for water limited conditions described by Van der Werf et al. (2004) forms the basis of this model. Several modifications had to be implemented to make the model applicable to mangrove ecosystems. First light use efficiency and fraction of intercepted light were removed, because the data set obtained from the meteorological department of Aruba did not include data on radiation, evaporation and transpiration. Instead, evapotranspiration was calculated according to the method of Hargreaves, which is based on minimum and maximum temperature. Hourly temperature observations were available for the period 2006-2016. Hence, ω is replaced by the potential crop evapotranspiration (ET_p).

In addition, a growth reduction term as a result of stress was implemented. This term is based on the stress parameters for water and salt stress. The parameter for water stress is dependent on the storage which is calculated using the terms of the water balance as given in equation 5, except for interception. Rainfall data was also included in the meteorological data set and thus available for the same period. However, no tidal data was available for Aruba, so the daily seawater inflow caused by tides was modelled. Estimations of the influx could be made using the information provided by online tides and currents predictor (Mobile Geographics, 2017). First the right location had to be selected, which was Willemstad (Curacao) since it lies closest to Aruba. Then the daily influx was calculated by subtracting low tide from high tide. Again, in case of multiple cycles during one day, the values were added together.

Furthermore, a growth efficiency term was added to the equation, otherwise growth would be unrestrained in absence of stress conditions. Finally, mortality was assumed to be a function of the stress instead of a fixed quantity. A mortality parameter was added to indicate the fraction of the biomass that is lost in case of stress. All these modifications resulted in the equations below (9 and 10), the different terms are described in detail in section 3.3.2.

$$\boldsymbol{B_t = B_{t-1} + \frac{dB}{dt}\Delta t} \tag{9}$$

where B_t is the above-ground biomass in kg and $\left(\frac{dB}{dt}\right)$ the change in biomass, which can be calculated according to equation 10:

$$\boldsymbol{\frac{dB}{dt} = MIN(\omega_w, \omega_s) * \varepsilon_w * ET_p * \left(1 - \frac{B_t}{B_x}\right) - a * B_t} \tag{10}$$

3.3.2 Tree growth and mortality parameters

Stresses

$MIN(\omega_w, \omega_s)$ is a dimensionless term indicating growth reduction due to either water or salinity stress. These two stresses, apart from nutrient and light availability, have to be taken into account in a mangrove type of environment. As water is the limiting factor for crop growth in semi-arid climate zones rather than radiation (Boyer, 1982), only water stress and salt stress are included. Nutrient limitation is beyond the scope of this study given the level of complexity (Alongi, 2009) and is therefore not included. The stress parameters (ω_w and ω_s) were calculated using the equations 3 and 4 in section 3.2 and are a measure of the growth limitation in case of stress.

Water use efficiency and (evapo)transpiration

Tree growth is calculated based on the relationship between transpiration and biomass growth. However, the amount of water that is required for CO_2 fixation differs per species and this, in turn, determines the amount of biomass that can be produced. The term in which this process is expressed is the water use efficiency (ϵ_w in equation 10) in kg biomass per l water transpired. Transpiration could not be measured during fieldwork. Consequently the soil evaporation was assumed to be negligible so the potential evapotranspiration (ET_p) could be used instead. The potential evapotranspiration can be derived from the reference evapotranspiration (ET_0) multiplied by the crop coefficient (FAO, 1998). Here a crop coefficient of a reference crop was used ($k_c = 1$).

Literature on water use efficiencies for mangrove species is mainly focussed on processes acting at the leaf scale. The water use efficiency (WUE) associated to the processes at this level of scale is also known as the intrinsic WUE. For the approach used in this study, however, the integrated WUE is needed. The integrated WUE is defined as the ratio of biomass produced to the rate of water that is transpired. Since the integrated WUE for mangroves is unknown, the WUE for C_3 crops is used alternatively. Penning de Vries (1989) found water use efficiencies for C_3 crops in the order of 0.0025 kg water per kg biomass.

Growth efficiency

The fourth term is referred to as the growth efficiency. Typically growth efficiencies decline in a stand's life span (Ryan et al., 1997), so this term cannot be disregarded when modelling tree growth. The growth efficiency here is calculated as a function of the biomass; the biomass at a given moment in time (B_t) is divided by the maximum biomass (B_x). The growth efficiency indicates to what extent the biomass production is reduced. It is a dimensionless value between 0 and 1, a growth efficiency of 1 means there is no reduction and 0 means there is no production. B_x is obtained from a review on mangrove productivity by Komiyama et al. (2008). In this paper the authors provide an overview of the worldwide biomass of mangrove forests. For *R. mangle* the maximum above-ground biomass (AGB) of 23.3 kg/m^2 was found for a 50-year-old forest stand in the Dominican Republic.

Mortality

All terms discussed above are related to the production of biomass, but it might be evident that multiple factors lead to a loss of biomass. In equation 10 biomass loss is indicated by the term $a * B_t$. Apart from senescence – which is implicitly incorporated in the growth efficiency – a major cause of natural losses in mangrove biomass can be attributed to environmental conditions, including water and salinity stress. In this model a denotes the reduction in biomass which is a function of stress and an arbitrarily chosen mortality parameter f_m (equation 11). This parameter indicates the fraction of the biomass that is lost and is set to 0.05.

$$\boldsymbol{a = (1 - MIN(\omega_w, \omega_s)) * f_m} \qquad \textbf{(11)}$$

4. Results

4.1 Hydrology of Spanish Lagoon

4.1.1 Freshwater supply

In figure 8 the distribution of the different components of the water balance is shown. In total nearly 327 mm of rainfall was measured between November and January. Over 20% of this amount was measured during an extraordinary rainfall event that occurred on November the 20th; almost 70 mm over a period of 6 hours. Compared to the monthly averages for the months November, December and January over the past 30 years, the monthly averages measured during fieldwork were considerably higher, especially in the months December and January when the averages were exceeded by 37 and 59 mm respectively.

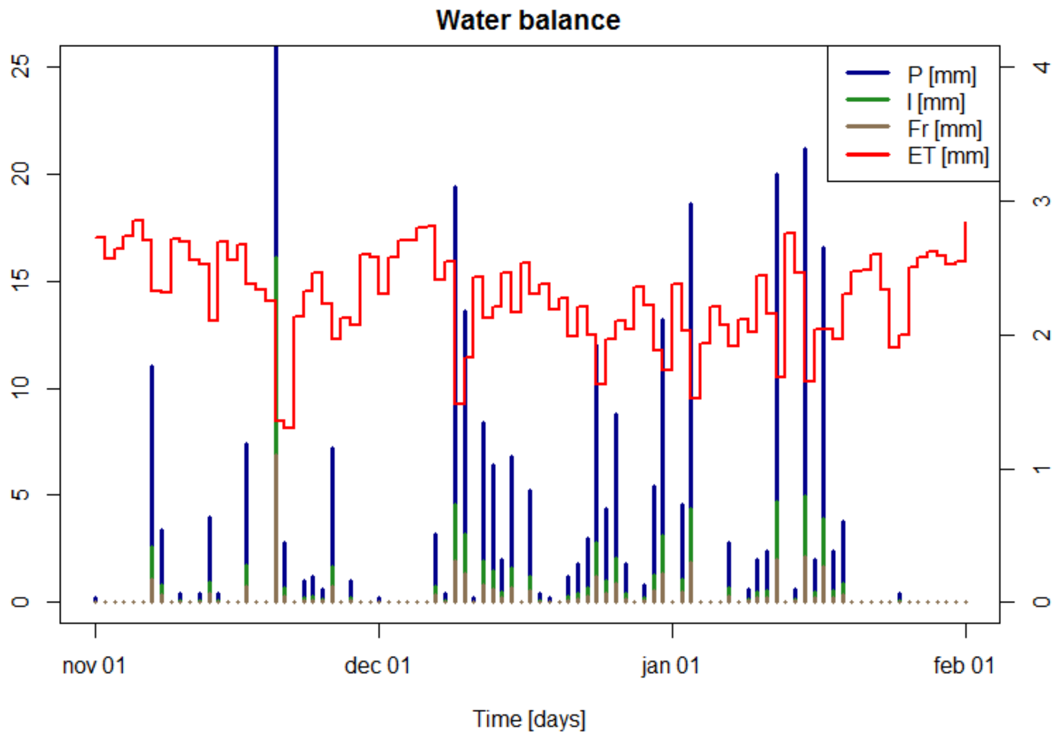

Figure 8 – Water balance for Spanish Lagoon during the fieldwork period. The left y-axis applies to the P, I and Fr and the right y-axis to the ET. The blue line represents the rainfall, the green line the rainfall interception, the brownish line the surface runoff and the red line the evapotranspiration.

Both rainfall interception and surface runoff are fixed fractions from the amount of precipitation and thus vary with the amount of precipitation. Surface runoff is another freshwater supplier and accounts for an additional 10% of the total amount of rainfall that enters the study area. By contrast, rainfall interception leads to a reduction in the freshwater supply. The average interception was determined based on 8 different rainfall events (n=24) and found to be 23% of the total amount of precipitation. In figure 9 the results of a linear regression analysis is shown. The R-squared, indicating the relation between the rain gauge and the throughfall gauges at each location, are fairly high; ranging from 0.85 for location 3 to 0.95 for location 4.

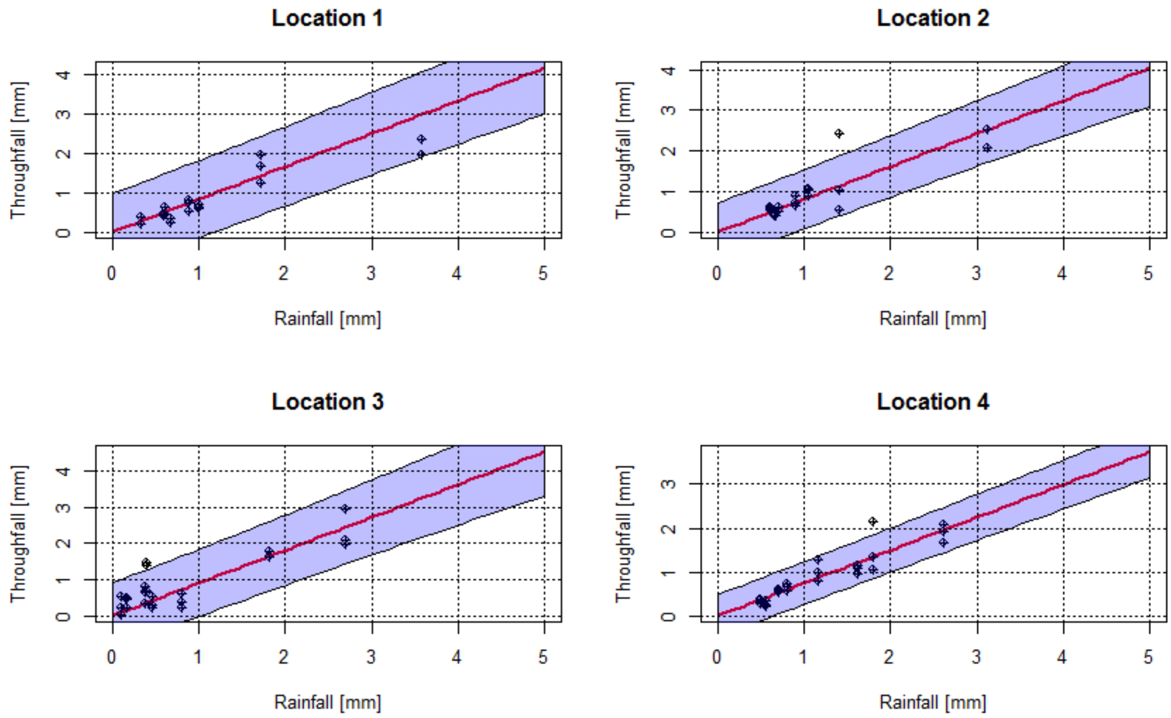

Figure 9 – Results of the linear regression analysis for rainfall interception as was measured at the different plots.

A second loss term is evapotranspiration. Unfortunately the evaporation measurements failed, so the evapotranspiration during the fieldwork period was calculated according to the method of Hargreaves. The average evapotranspiration over this period is estimated on 2.3 mm/d. In addition to the automatic measurements by the pressure sensor also manual measurements of the water height in the pan were carried out for one month. From these measurements the evaporation could be derived and converted to evapotranspiration by means of the pan coefficient. A qualitative comparison between the calculated and the measured evaporation shows that the measured values fluctuate considerably more than the calculated values (figure 2 in the annex). The calculated ET ranges from 1.5-2.5 mm/d, whereas the measured ET ranges from 1 and 5 mm/d.

4.1.2 Seawater inflow

Figure 10 shows the results of the tide measurements. The four divers that were installed in the canal in front of the forest more or less display the same pattern. However, as can also be noticed from this figure, “Diver 5” – which was installed on the landward side of the forest (i.e. the hinterland) – significantly differs from the measurements in the canal and shows a more irregular pattern. This suggests that the influence of tides is decreased in the hinterland. The water heights in the canal fluctuate 20 to 30 cm depending on the strength of the tides, whereas the difference in water height due to tides in the hinterland occasionally fluctuates more than 5 cm.

The salt concentration of the seawater was measured multiple times, both during both high and low tide, once after a rainfall event and two times randomly. On average the electrical conductivity was around 56 mS/cm, which corresponds very well to EC values for seawater found in literature, which are in the order of 55 mS/cm (CWT 2004). The boxplot in the annex (figure 3) provides an overview of the variation in the measurements. It can be noticed that the variation was largest just after a rainfall event.

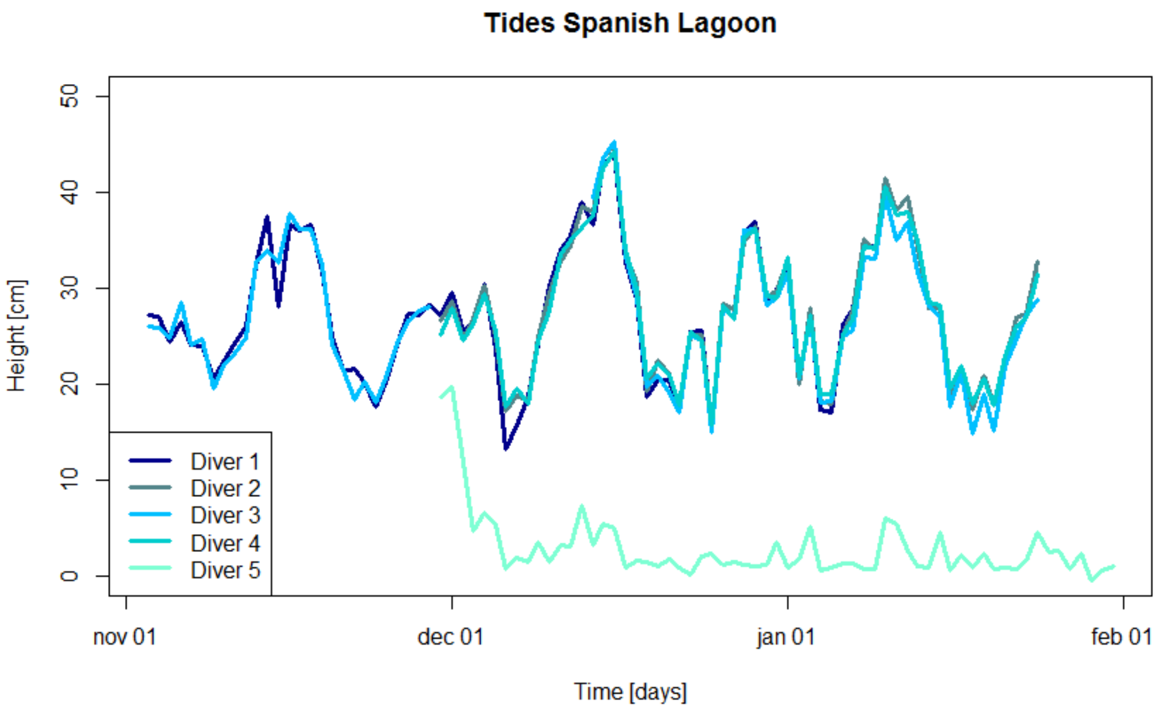

Figure 10 – The effect of tides measured at five different locations in the study area based on diver data; the first 4 divers were installed in the canal, the last diver was installed in the hinterland.

For the modelling of mangrove biomass, tides were modelled for the simulation period. A simple validation was performed between the measured tides and the modelled tides during the fieldwork period in order to get an impression of the model performance. The results of this validation can be found in figure 4 in the annex. It appears that the modelled tides correspond fairly well to the measured tides

4.1.3 Growth conditions during fieldwork

The stress parameters for the head of Spanish Lagoon are shown in figure 11. Neither water nor salt stress occurred in the tail during the fieldwork period. Hence, the growth performance is 1, because the combined effect of the stresses does not lead to growth reduction. In the head no reduction as a result of salt stress occurred. However, the parameter for water stress occasionally dropped below 1, especially during the last few days of the fieldwork period (see figure 11).

For the initial salt concentration of the soil, the results obtained by the saturated paste method for the head as well as the tail were used. The average salt concentration found for the head was 11.1 kg/m^2 and 7.2 kg/m^2 for the tail. However, variation is quite large as can be seen in the boxplot (figure 5 in the annex), especially in case of the transect along the tail; at some locations the EC is close to zero, whereas at other locations the EC reaches values of around 70 mS/cm.

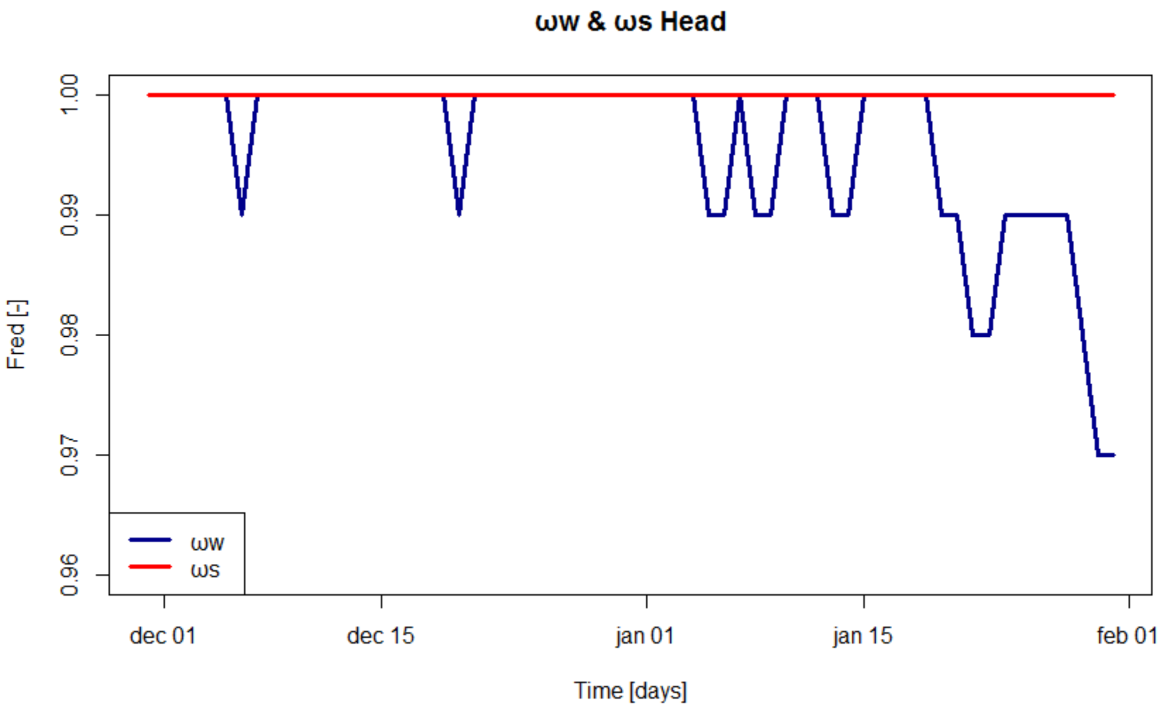

Figure 11 – Stress parameters for both water stress and salt stress in the head of Spanish Lagoon. The blue line indicates to extent of water stress and the red line to extent of salt stress.

4.2 Modelling mangrove biomass

4.2.1 Current biomass

The results with respect to the DBH measurements can be found in table 1. In total 24 trees were monitored and the average biomass of all trees was 99.8 kg/tree. There is quite some variation between the different locations; the above-ground weight of the trees ranges from 18.9 to 331.9 kg/tree. At the first three locations the variability in tree size was larger than at location 4. The average tree density for all monitoring plots was estimated as 0.1 tree per square meter.

Location	Distance from open sea [m]	Number of trees	Average AGB [kg]	Average AGB [kg/m^2]	Average LAI
1	1250	6	71.3	7.1	2.21
2	1130	6	52.3	5.2	2.37
3	1000	6	82.9	8.3	2.04
4	580	6	192.6	19.3	2.00

Table 1 – The average above-ground biomass for each monitoring plot.

The average LAI per plot is also given in table 1 and varies from 2.00 for plot 4 to 2.37 for plot 2. The average LAI of all four plots was used to calculate the crop coefficient, which appeared to be circa 0.9. In total 25 photographs were taken to determine the average LAI. The extinction coefficient for both *R. mangle* and the reference crop was assumed to be 0.65.

In table 2 an overview is given of AGB data for *Rhizophora* species (spp.) based on review articles by Saenger and Snedaker (1993) and Komiyama et al. (2008). In addition, information on latitude, species composition (i.e. mixed or monoculture) and condition/age (if known) is provided. The average biomass found for location 4 compares reasonably well to the biomass found in India for *Rhizophora* spp. Biomass measured at location 1-3 correspond quite well to the amount of biomass found for forests in Sri Lanka and Puerto Rico. Especially the results found in Puerto Rico are interesting, since these represent a forest which is completely composed of *R. mangle*, like the trees monitored in Spanish Lagoon.

Region	Latitude (°)	Species	Condition/age	AGB [kg/m^2]	Source
Dominican Republic	19.1	*R. mangle*	50 years	23.3	Komiyama et al. (2008)
Puerto Rico	18.0	*R. mangle*	-	6.3	Komiyama et al. (2008)
Thailand	9.0	*Rhizophora spp*	Primary forest	28.1-29.9	Komiyama et al. (2008)
Sri Lanka	8.2	*Rhizophora spp*	Island habitat/ fringe	7.1-24.0	Komiyama et al. (2008)
India	12.0	*Rhizophora spp*	Primary forest	21.4	Komiyama et al. (2008)
French Guiana	5.3	*Rhizophora spp.*	Matured coastal/riverine	12.2-31.5	Komiyama et al. (2008)
Indonesia	1.2	*Rhizophora spp*	-	17.8-43.6	Saenger & Snedaker (1993)
Malaysia	5.0	*Rhizophora spp*	-	14.7-31.4	Saenger & Snedaker (1993)
Thailand	8.0	*Rhizophora spp*	-	15.9	Saenger & Snedaker (1993)
Panama	9.0	*Rhizophora spp*	Primary forest	27.9	Saenger & Snedaker (1993)
Japan	24.0	*Rhizophora spp*	-	9.8-10.8	Saenger & Snedaker (1993)
USA (Florida)	26.0-27.3	*Rhizophora spp*	-	0.8-16.4	Saenger & Snedaker (1993)

Table 2 – Overview of the AGB of *Rhizophora spp.* in different countries. Data was particularly selected for *Rhizophora spp.* from reviews by Komiyama et al. (2008) and Saenger and Snedaker (1993).

4.2.2 Future biomass (modelling)

The model results concerning biomass production in Spanish Lagoon are presented in figure 12 and 13. The black lines show the biomass production under the current conditions. As becomes clear from these lines, both the AGB in the tail and in the head of Spanish Lagoon reach equilibrium levels towards the end of the simulation period. This indicates that after 10 years tree growth is nearly compensated by mortality and that the maximum biomass is reached.

Reduced seawater inflow in the hinterland might occur and is caused by the larger slope in the hinterland compared to the inlet or by blocking mechanisms (e.g. due to growth). As a consequence the salt concentration increases. In case the seawater inflow is reduced by 25% tree growth is not limited (figure 13). The implications of two other scenarios on production in case of reduced seawater inflows are also shown in this figure. It can be noticed that growth in the hinterland is reduced considerably or even impossible as a result of increased salt concentrations. Given the salt tolerance of *R. mangle*, which corresponds to an EC that is twice EC of seawater, salt concentrations in the head are at least twice the concentration of seawater.

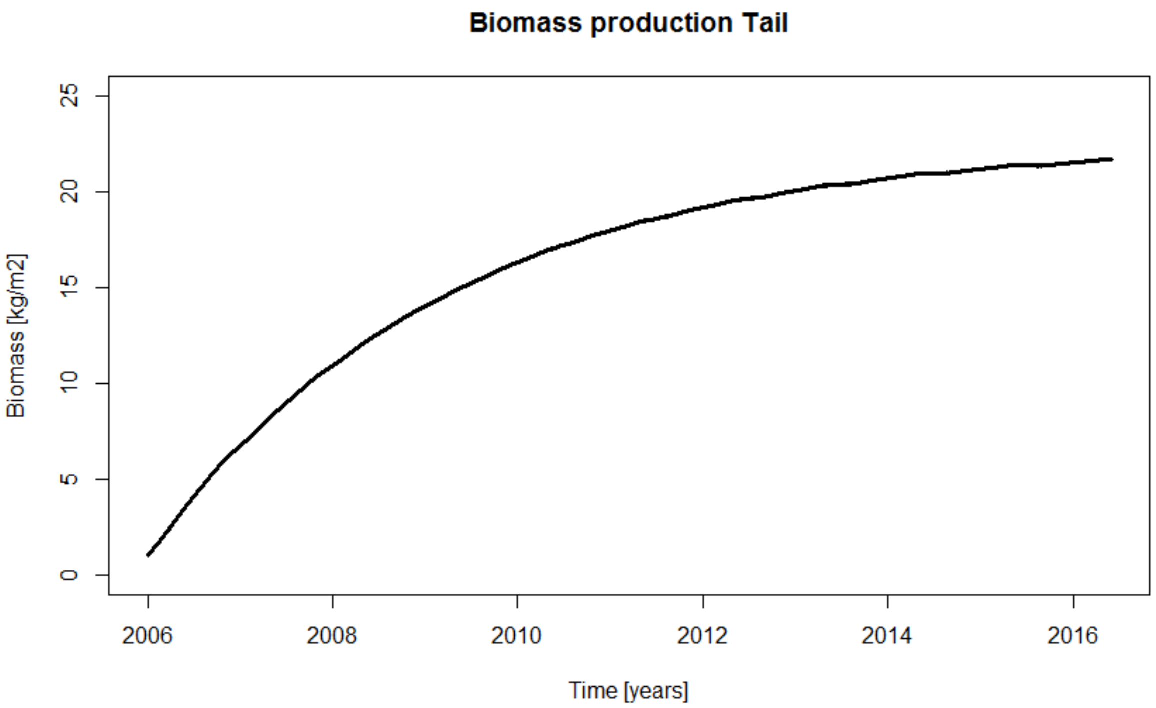

Figure 12 –Simulation of the biomass production in the tail of Spanish Lagoon under the current hydrological conditions.

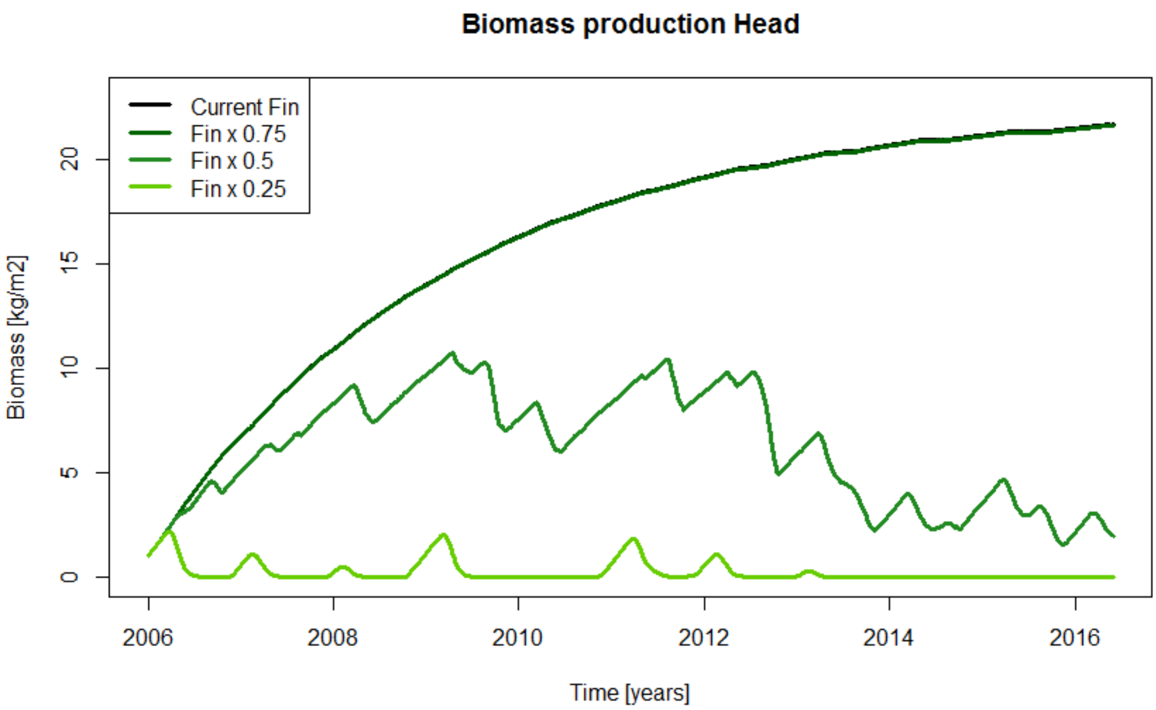

Figure 13 – Simulations of biomass production in the head of Spanish Lagoon for the current hydrological conditions (black line) as well as for reductions of seawater inflow by 25%, 50% and 75% (dark green, middle green and light green line respectively). The dark green line coincides with the black line.

The influence of surface runoff on production in case of growth limitations is shown in figure 14. The production under a reduction of the tides by 50% was taken as an example. The extent to which runoff can contribute to an enhanced tree growth for this particular example is simulated for different runoff fractions. The current fraction ("Rn", indicated by the black line in figure 14) is 10% of the amount of rainfall, two higher fractions are added ("R 15%" and "R 20%", indicated by the dark and middle green line respectively) and one lower fraction is added ("R 5", indicated by the light green line). The latter corresponds to model results of a study by Kuppen (2017). He found that the amount of surface runoff during the extreme event on November the 20th was 39800 m^3 over an area of 13 km^2. This comes down to a fraction close to 5% of the total amount of rainfall.

The differences in biomass productions for the different scenarios are minimal as becomes clear from the results provided by figure 14. Differences are largest in the middle section of the graph, where the biomass production in case of "R 20%" is around 1 kg/m^2 higher than for "R 5%". However, for the first and the last couple of years of the simulation period the biomass production is approximately the same.

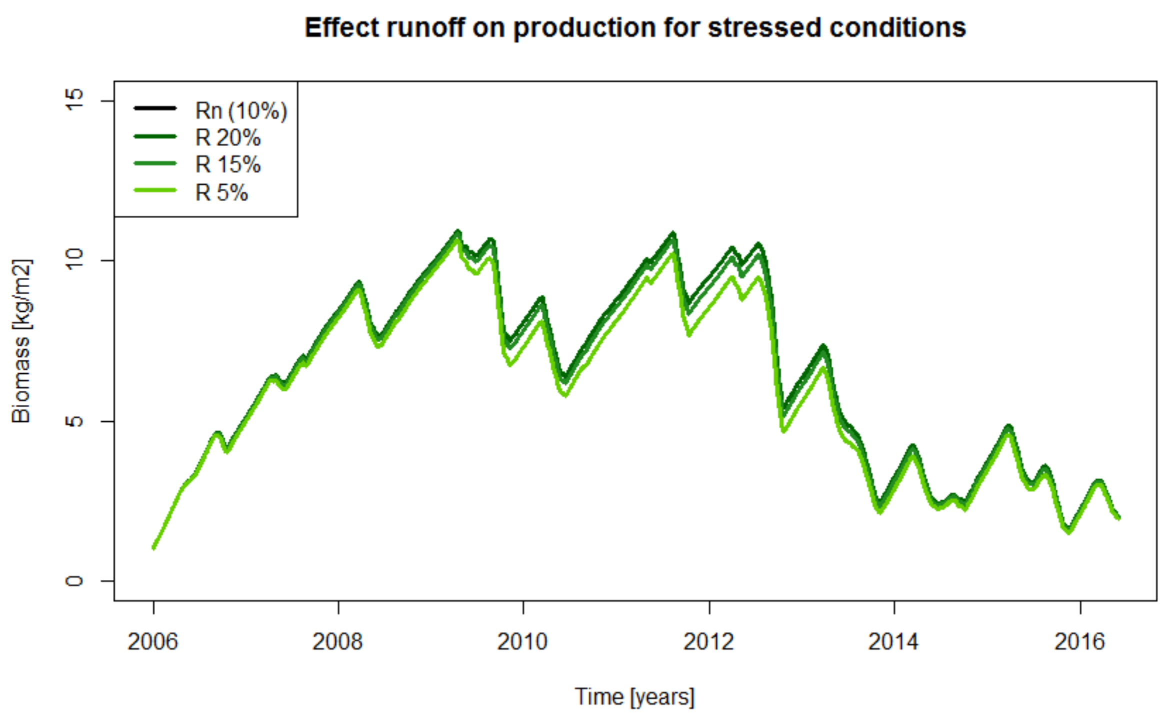

Figure 14 – Effect of surface runoff on biomass production for stressed conditions; each line represents the biomass production based on four different fractions for surface runoff.

4.2.3 Parameter sensitivity analysis

In addition to the analysis of the model's sensitivity to changes in hydrological conditions also a parameter sensitivity analysis for the tree growth model was performed. This was done for one parameter, the WUE, under the current hydrological conditions (figure 15) as well as under stressed conditions (figure 16). As an example of stress conditions a reduction of the tides by 50% was taken. Note that figure 15 applies to both the head and the tail, whereas figure 16 only refers to the head. The red line indicates the biomass production for a water use efficiency of 0.0025, which is considered to be the mean. The blue lines are 50 possible values for the WUE that deviate from the mean WUE within a margin of 10%.

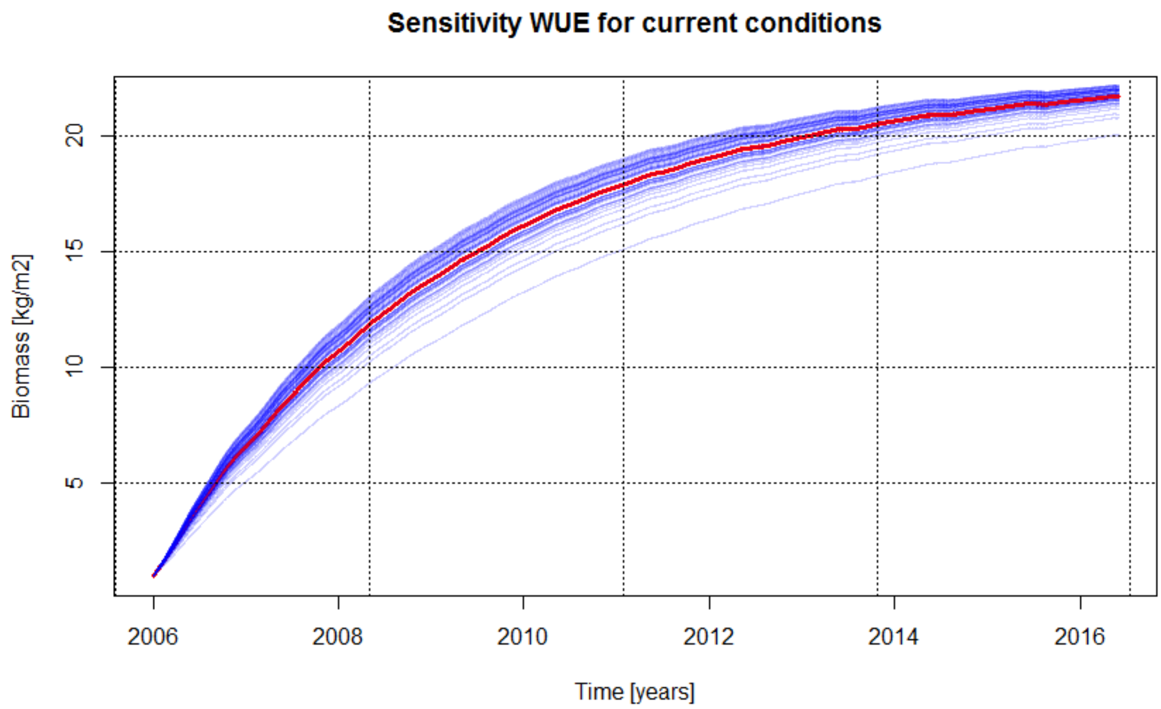

Figure 15 – Model sensitivity to different WUEs under the current hydrological conditions (at full tide)

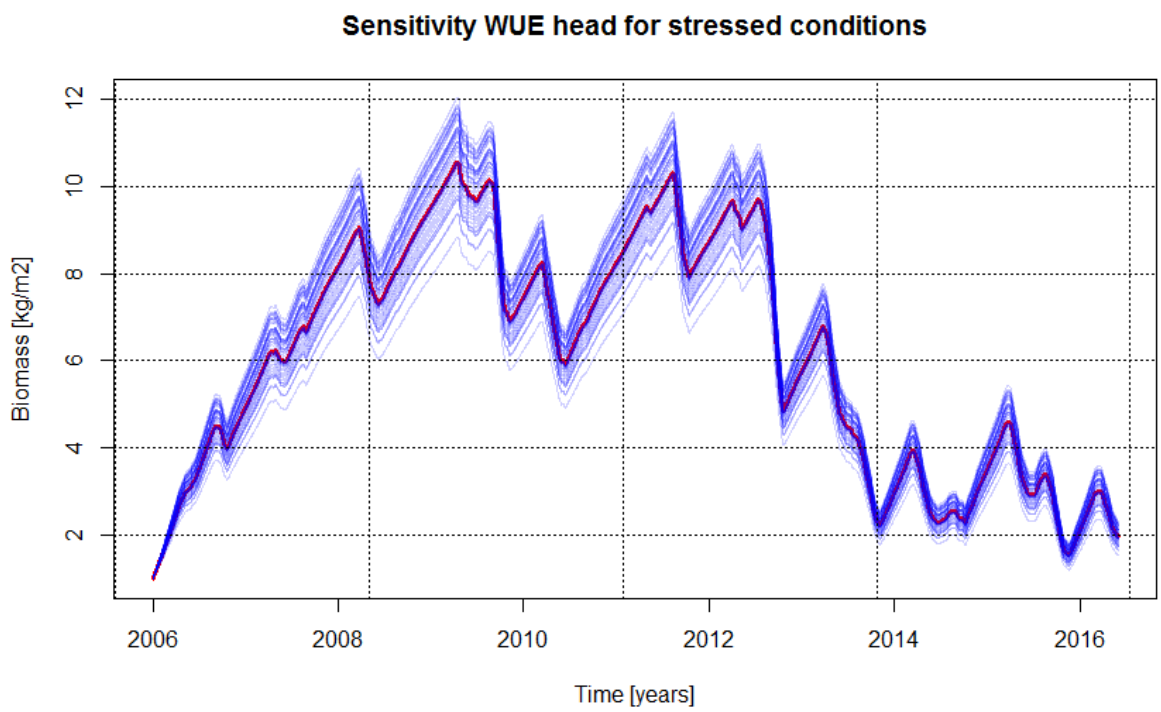

Figure 16 – Model sensitivity for different WUEs under stressed conditions (at 50% tide)

From the trends of all possible WUEs for the current conditions it appears that in the long run the maximum biomass will be reached ultimately. However, the time it takes to reach equilibrium differs per simulation and varies in the order of years for the two most extreme values. In case of stressed conditions the trends in the amount of biomass per square meter are equal, but the absolute amounts differ considerably especially over the period 2007-2012, varying around 3.5 kg/m^2 for the most extreme values. At the end of the simulation period there is no distinct difference in the amount of biomass between the minimum and maximum WUE.

5. Discussion

5.1 The current status

The current AGB for *R. mangle* found in this study compares fairly well to averages found in other regions (Saenger and Snedaker, 1993; Komiyama et al., 2008). An important factor in this comparison is the latitude. Saenger and Snedaker (1993) found that heights of the canopy increased towards the equator. Consequently, the AGB of primary and mature forests in low latitudes is generally high. This becomes clear from the overview provided in table 2, in which the average AGB of *Rhizophora* species is given for different regions. For a fair comparison the age or conditions of the forest should also be taken into account, however this is not always documented.

According to Komiyama et al. (2008) the AGB increases in landward direction. This is in agreement with field observations. Although, the fourth measurement location suggests that the AGB is higher in seaward direction, it should be mentioned that in the hinterland mainly younger trees were selected for DBH measurements; trunks of younger trees are often rather straight compared to those of older trees. For DBH measurements straight trunks are preferred, since the measurements can be performed more accurately. So, in fact, the average biomass at the first tree plots might be higher than appears from the results. Moreover, the density was estimated for the entire study area based on photographs, but in reality the density differed per plot. Densities seemed to be higher for the first three plots. Clearly age could also play a role, as younger trees were mainly found in the hinterland.

Furthermore, the results of both the water and the salt balance underline that the current status of the forest in terms of biomass production is comparable to those in other regions under the current hydrological conditions. This can be concluded from the stress parameters, which indicate that neither water nor salinity stress occurred during the fieldwork period in the tail. Only a minor potential for reduction (<5%) occurred in the hinterland due to shortage of water in the last two weeks of the fieldwork period. However, the measurements and analyses in this study are focussed on *R. mangle*, whereas the forest on the landward side is mainly composed of *A. germinans*. Chen and Twilley (1998) found that *A. germinans* have a higher salt tolerance, which might imply that growth in the hinterland is not limited at all. It would be advisable to verify this based on a long-term monitoring study on the growth of both species.

The results for the LAI were rather questionable and thereby the crop coefficient as well. This could be caused by the type of lens that was used to make the hemispherical photographs. Typically, lenses for smartphone cameras have FOV smaller than 180°. As a consequence the photographs could not be analysed properly using the GLA and this probably resulted in an underestimation of the LAI. Moreover, the projection distortion of the lens is unknown. Therefore, the K_c of a reference crop was used for calculating the potential crop evapotranspiration. As a matter of fact it would be better to find a crop coefficient for mangroves specifically.

5.1.1 Contribution of freshwater supply

The changes in water levels as a result of tides are considerably lower in the hinterland compared to those measured in the canal. The effect of tides in the hinterland is approximately reduced by a factor 9, which implies that the salt water supply here is significantly lower. Presumably the water flow is blocked by the forest that separates the hinterland from the canal. As a consequence of sediment accumulation in the forest, the maximum water depth was around 40 cm – except for a small channel that connected the canal with the hinterland – whereas the water depth at the end of the canal was around 2m. Because of the reduced seawater supply the influence of other water resources (e.g. precipitation, surface runoff and groundwater flow) on tree growth in the hinterland of Spanish Lagoon were also evaluated.

Rainfall varies among the seasons as well as on annual basis (Giannini et al., 2000). The amounts measured during the fieldwork period are a good example of this; rainfall in the months November, December and January was above average. Two other resources – indirectly related to rainfall – also contribute to the water supply in the hinterland, which are groundwater flow and surface runoff. However, groundwater flow in semi-arid climates is only a temporary resource, since the potential evapotranspiration exceeds precipitation most of the time (Van Sambeek et al., 2000). Although, mangroves need a constant water supply. In addition, the sensitivity analysis shows that the contribution of surface runoff is not significant; despite increased amounts of surface runoff during stress conditions the amount of biomass gradually declines, so mangroves are slowly dying. Moreover, both groundwater flow and runoff contribute mainly during the rainy season. In these periods both water stress and salt stress are not likely to occur. This suggests that contribution of these terms is not determining in long-term mangrove growth. However, trees might exhibit seasonal diameter growth patterns, since growth is correlated to the presence of seasonally available supply of freshwater (Krauss et al., 2006).

5.2 Future perspectives

In addition to the results regarding the current status of the forest, the model results also indicate that future tree growth under the current hydrological regime is not limited; the AGB increases over a period of 10 years towards the maximum biomass both in the head and the tail of Spanish Lagoon. Based on the results of the tidal data, different scenarios of reduced seawater inflow were evaluated. In case the seawater inflow is reduced by 50%, the production is reduced considerably with respect to the production under the current seawater inflow. Initially growth occurs, but the growth is limited to a biomass of 10 kg/m^2, which is nearly half of the maximum biomass without stress. However, mortality occurs during the last 3 years of the simulation period. For this scenario the effect of surface runoff was also evaluated. As can be concluded from figure 13 a higher surface runoff obviously leads to slightly less reduction, however it can clearly not prevent the trees from mortality. For the last scenario, where the seawater inflow is a quarter of the current inflow, growth is impossible.

Overall, the results indicate that maintenance is necessary such that tidal currents reach further landward. Without maintenance mangroves will also occupy the channel. As a consequence sediments will accumulate and the water supply to the hinterland declines until the flow is eventually blocked. Deepening of the channel would be a good measure since the slope, which is one of the reasons tides extinguish, is decreased and therefore the inflow is larger.

Recently, an S-shaped channel was dug in the hinterland, which has a length of 150m and a total width of 20m (DCNA, 2017). This project is part of a restoration plan – in which Wageningen Environmental Research (Alterra) was involved – to compensate for the loss of mangroves due to the construction of a new bridge. At low tide the water depth in the channel will still be around 50cm.

Given the fact that tides reach further inland as a result of this measure, it is expected that the forest will have the potential to extend in landward direction. The model results support this expectation. However, a study by Kuppen (2017) shows that the amount of sediments transported to the hinterland of Spanish Lagoon during high intensity rainfall events is in the order of magnitude of 338 tons, which is around 20% of the total volume of the new channel. This indicates that the implications of sedimentation on tree growth should also be investigated, especially because the model results have a high uncertainty.

Furthermore, it is expected that climate change will have positive effects on mangrove growth in the hinterland of Spanish Lagoon given the fact that seawater will reach further inland. Predictions of climate change for the Caribbean islands namely show that sea level will rise with a rate of 3-5 mm/year over the next century (IPCC, 2001). Findings by McKee et al. (2007) support this expectation, they found that Caribbean mangroves adjust to rising sea level. However, the implications of climate change on tree growth in Spanish Lagoon should be reviewed in more detail.

5.3 Model characteristics and limitations

5.3.1 Model validation

A comparison between the measured biomass and modelled biomass shows that the model results are not completely in accordance with the measured amounts of biomass. The measured AGB at location 4 (19.3 kg/m^2) comes closest to the modelled biomass ($\sim$23 kg/m^2). Again, this can be explained by age of the trees that were monitored at the other plots; trees were relatively young at these plots, whereas plot 4 mainly consisted of mature trees. It should be noted that the density needs to be determined more accurately in order to come up with a more reliable estimates for the AGB. The model clearly needs to be validated more thoroughly to assess its performance. This could be done by applying the model to forests that are monitored for over a longer period, such that estimates of the AGB and the tree density should be quite reliable. An additional check would be to apply the model to other mangrove forests in the Caribbean in order to evaluate whether the results are comparable.

5.3.3 Parameter uncertainty

Parameter uncertainty can have a significant effect on the model results. Therefore, a sensitivity analysis has been performed for the water use efficiency. Uncertainty in water use efficiency leads to a large effect on the biomass production as can be seen in figure 15; the time it takes to reach maximum biomass differs in the order of years. The impacts of uncertainty become smaller for situations where growth is limited.

The model is also sensitive to changes in hydrological fluxes as well as stress parameters (parameter b) and other tree growth parameters, for example the maximum tree biomass, crop coefficient and mortality rate. These parameters are either based on estimates (B_x and f_m), on reference values ($K_c = 1$) or assumptions (parameter b), so it would be interesting to analyse in the effect of these parameters on the model results. Given the fact that the model was built in excel a sensitivity analysis for all parameters was rather inconvenient to perform, therefore a combined analysis is not included in this study.

5.3.3 Measurement uncertainty

Finally, measurement errors also affect the model results. For that reason interception is not included in the model. The results need to be verified first. Additional research to the effect of intensity and duration, but also canopy cover is required for mangrove species specifically. Furthermore, it should be mentioned that the last measurement location was not included in the regression analysis, since the bottles were not filled by rainwater only, but also by seawater as a result of waves.

A comparison between the measured and calculated ET_0 also shows that the variation of the evapotranspiration is in fact larger. Gavilán et al. (2006) evaluated the performance of ET_0 calculated by Hargeaves in a semiarid climate. They compared the results to the standard calculations for ET_0 (Penman-Monteith) and found that the ET_0 was generally underestimated close to the coast. It would therefore be interesting to quantify the ET_0 more accurately to assess the effect on tree growth.

Another method that was quite prone to measurement errors was the saturated paste method. The water quantities extracted from the samples were very low and hence the EC of the samples was hard to measure. This implies that the initial salt content of the soil could have been be either higher or lower. We expect the effect on the results to be negligible, since the salt concentration in the soil is close to the concentration of seawater as long as the inflow is sufficient, which is the case under the current hydrological conditions.

Finally, changes in storage can have minor implications on the results. It determines the amount of water which can be stored in the soil and thus the amount of water that is potentially available for mangroves. Estimations of the depth of the sediment layer, in which mangroves are rooted, were quite hard to make, mainly due to the lack of proper tools (e.g. a gouge). The largest depth that was measured was 2m, but the actual maximum depth remains unknown. Additionally, soil texture is hard to determine for sediments in which mangrove are rooted. Samples were taken of the sediments located next to the water (at sites that were occasionally flooded), hence values found for the conductivity and the available water content might not be representative. However, the results do not indicate that under the current conditions tree growth is sensitive to changes in storage.

6. Conclusion and recommendations

This study shows that the current hydrological conditions are favourable for mangrove growth, both in the head and the tail of Spanish Lagoon. The effect of tides in the hinterland is considerably reduced compared to the effect observed near the inlet; the seawater inflow in the hinterland is approximately 10% of the inflow near the inlet. Regardless of the reduced seawater inflow in the hinterland, the current inflow is still sufficient to prevent mangroves from both water and salinity stress.

Overall, the average above-ground biomass of *Rhizophora mangle* measured in Spanish Lagoon is comparable to averages measured in other forests at approximately the same latitude. Additional research is required to determine whether this is also the case for *Avicennia Germinans*. In such a study it is important to include information on the age or condition of the forest as well as on tree density and heights. Long-term monitoring of the trees would also provide more insight in the dynamics of this forest and could be useful to detect and adapt to changes.

This study provides a model that is widely applicable because of its simplicity. However, it needs to be validated in order to assess its performance. This could be done by applying the model to other regions. The model results of indicate that a large (>50%) reduction of the seawater inflow is the greatest threat for the mangrove forest in Spanish Lagoon. A reduced inflow would increase the salt concentration in the hinterland and could eventually result in mortality. Therefore, maintenance is necessary to keep the hinterland in connection with the canal such that the seawater inflow is sufficient to counter salinization of the hinterland. However, it can be concluded that under the current hydrological conditions the habitat function of Spanish Lagoon is not in danger.

The contribution of other water resources is not crucial for tree growth. Groundwater flow and surface runoff are only temporary resources, whereas mangroves need a constant water supply. The model results show that increased amounts of surface runoff lead to a slightly higher AGB, but in case of stress trees will die ultimately. The contribution varies among the seasons as well as on annual basis. The amount of rainfall during the fieldwork period, for example, was above average. In addition, groundwater flow and surface runoff contribute in wet periods, in which stress is not an issue.

The effect of sedimentation was not evaluated in this study. A modelling study by Kuppen (2017) indicates that the amount of sediments transported to Spanish Lagoon during high intensity rainfall events is quite large. However, considering the large uncertainty of the model additional research is required to study the effect of sedimentation on tree growth more accurately to evaluate the impacts. The effects of climate change are not included in this study. It is expected that climate change has a positive effect on tree growth, since predictions indicate that sea levels will rise in the Caribbean. However, additional research is necessary to evaluate these predictions more thoroughly.

Finally, a sensitivity analysis shows that the effect of parameter uncertainty on the model results is rather considerable; the growth rate can be reduced by 2 years. Only the effect of uncertainty of the water use efficiency was evaluated. However, it is definitely useful to investigate the combined effect of all model parameters with regard to the sensitivity of tree growth to changes in parameter values. Different approaches can be used to evaluate the effect of parameter uncertainty and explain the variation in biomass as a results of the variation of one parameter. For such an analysis the methods like the Sobol sequence described by Sobol (1993) and the Latin Hypercube described by McKay et al. (1979). The model can also be improved by finding more specific parameters for mangroves, like the integrated WUE and the crop coefficient. Tree growth simulations would consequently be more realistic.

7. Acknowledgements

My time at Aruba was unforgettable: the people were very friendly, the food was great and the weather was nice. All this really motivated me during my research. I would like to thank several people who contributed to my research. First of all, I would like to thank Emil ter Horst for his hospitality, assistance and the good coffe during the fieldwork period at Aruba. He was always willing to help to tackle problems. I also want to thank Teun and Anouk as well, who made it a whole lot easier for me to carry out my measurements. Finally, I want to thank Daniel van de Craats for providing the model to simulate tides.

8. References

Allen, R.G.; Pereira, L.S.; Raes, D.; Smith, M. Crop evapotranspiration. Guide-lines for computing crop water requirements. In *FAO Irrigation and Drainage Paper 56*; FAO: Rome, 1998. http://www.fao.org/docrep/x0490e/x0490e00.htm

Alongi, D. M. (2008). Mangrove forests: resilience, protection from tsunamis, and responses to global climate change. *Estuarine, Coastal and Shelf Science*,*76*(1), 1-13.

Alongi, D. (2009). *The energetics of mangrove forests*. Springer Science & Business Media.

Ball, M. C. (1988). Ecophysiology of mangroves. *Trees*, *2*(3), 129-142.

Boyer, J. S. (1982). Plant productivity and environment. *Science*, *218*(4571), 443-448.

Calderon, H., Weeda, R., & Uhlenbrook, S. (2014). Hydrological and geomorphological controls on the water balance components of a mangrove forest during the dry season in the Pacific Coast of Nicaragua. *Wetlands*, *34*(4), 685-697.

Chen, R., & Twilley, R. R. (1998). A gap dynamic model of mangrove forest development along gradients of soil salinity and nutrient resources. *Journal of Ecology*, *86*(1), 37-51.

Clean Water Team (CWT) 2004. Electrical conductivity/salinity Fact Sheet, FS-3.1.3.0(EC). in: *The Clean Water Team Guidance Compendium for Watershed Monitoring and Assessment, Version 2.0*. Division of Water Quality, California State Water Resources Control Board (SWRCB), Sacramento, CA.

Clough, B. F. (1984). Growth and salt balance of the mangroves Avicennia marina (Forsk.) Vierh. and Rhizophora stylosa Griff. in relation to salinity.*Functional Plant Biology*, *11*(5), 419-430.

Danielsen, F., Sørensen, M. K., Olwig, M. F., Selvam, V., Parish, F., Burgess, N. D., Hiraishi, T., Karunagaran, V.M., Rasmussen, M.S., Hansen, L.B., Quarto, A. & Suryadiputra, N. (2005). The Asian tsunami: a protective role for coastal vegetation. *Science(Washington)*, *310*(5748), 643.

de Buisonjé, P. H. (1974). *Neogene and quaternary geology of Aruba, Curacao, and Bonaire* (No. 78). Utrecht.

DCNA, 2016. Dutch Caribbean Nature Alliance. Spanish Lagoon. Retrieved on 21 September 2016. http://www.dcnanature.org/spanish-lagoon/

DCNA, 2017. Dutch Caribbean Natura Alliance. Aruba: mangrove restoration begins at Spaans Lagoen. Retrieved on 28 June, 2017. http://www.dcnanature.org/mangrove-restoration-spaans-lagoen/

Decagon devices, Pullman, WA. Hydraulic Conductivity. *Mini disk portable tension infiltrometer*. Retrieved on 25 June 2017. http://www.decagon.com/en/hydrology/hydraulic-conductivity/mini-disk-portable-tension-infiltrometer/

Departemento Meteorologico Aruba, 2016. Climate Data Aruba. Retrieved on 22 September 2016. http://www.meteo.aw/climate.php

Devoe, N. N., & Cole, T. G. (1998). Growth and yield in mangrove forests of the Federated States of Micronesia. *Forest Ecology and Management*, *103*(1), 33-48.

Dirksen, C. (1999). *Soil physics measurements*. Catena Verlag.

Downton, W. J. S. (1982). Growth and osmotic relations of the mangrove Avicennia marina, as influenced by salinity. *Functional Plant Biology*, *9*(5), 519-528.

Duke, N. C. (1993). Mangrove floristics and biogeography. *Tropical mangrove ecosystems*, 63-100.

Erwin, K. L. (2009). Wetlands and global climate change: the role of wetland restoration in a changing world. *Wetlands Ecology and management*, *17*(1), 71-84.

FAO (1994). Agriculture Organization of the United Nations. Forest Resources Development Branch. (1994). *Mangrove Forest Management Guidelines* (Vol. 117). Food & Agriculture Org. http://www.fao.org/docrep/016/ap428e/ap428e00.pdf

FAO (2003). Status and trends in mangrove area extent worldwide. In: Wilkie, M.L. & Fortuna, S., eds. *Forest Resources Assessment Working Paper No. 63*. Rome: Forest Resources Division, FAO. http://www.fao.org/docrep/007/j1533e/J1533E00.htm

FAO Training Series, 2017. Soil. Chapter 6 Soil Texture. 6.2 *How to find the approximate proportions of sand, silt and clay*. Retrieved on 12 January 2017. ftp://ftp.fao.org/fi/cdrom/fao_training/fao_training/general/x6706e/x6706e06.htm#top

Frazer, G. W., Canham, C. D., & Lertzman, K. P. (1999). Gap Light Analyzer (GLA), Version 2.0: Imaging software to extract canopy structure and gap light transmission indices from true-colour fisheye photographs, user's manual and program documentation. *Simon Fraser University, Burnaby, British Columbia, and the Institute of Ecosystem Studies, Millbrook, New York*, *36*.

FWT Penning de Vries. (1989). *Simulation of ecophysiological processes of growth in several annual crops* (Vol. 29). Int. Rice Res. Inst..

Gavilán, P., Lorite, I. J., Tornero, S., & Berengena, J. (2006). Regional calibration of Hargreaves equation for estimating reference ET in a semiarid environment. *Agricultural Water Management*, *81*(3), 257-281.

Giannini, A., Kushnir, Y., & Cane, M. A. (2000). Interannual variability of Caribbean rainfall, ENSO, and the Atlantic Ocean. *Journal of Climate*, *13*(2), 297-311.

Gondwe, B. R., Hong, S. H., Wdowinski, S., & Bauer-Gottwein, P. (2010). Hydrologic dynamics of the ground-water-dependent Sian Ka'an wetlands, Mexico, derived from InSAR and SAR data. *Wetlands*, *30*(1), 1-13.

Grontmij & Sogreah, 1968. Water and land resources development plan for the islands of Aruba, Bonaire and Curacao. Volume B inventory of land and water resources. Report Grontmij (De Bilt): 133 pp.

Imbert, D., Rollet, B., 1989. *Phytmassaerienne et production primaire dans la mangrove du Grand Cul-de-sac Marine (Guadeloupe, Antilles francaises)*. Bull. Ecol. 20, 27–39.

IPCC (2001). *Climate change 2001: the scientific basis.* Contribution of Working Group I to the Third Assessment Report of the Intergovernmental Panel on Climate Change. Cambridge University Press, Cambridge.

Jimenez, J. A. (1992). Mangrove forests of the Pacific coast of Central America. *Coastal plant communities of Latin America*, 259-267.

Komiyama, A., Ong, J. E., & Poungparn, S. (2008). Allometry, biomass, and productivity of mangrove forests: A review. *Aquatic Botany*, *89*(2), 128-137.

Krauss, K. W., Keeland, B. D., Allen, J. A., Ewel, K. C., & Johnson, D. J. (2007). Effects of season, rainfall, and hydrogeomorphic setting on mangrove tree growth in Micronesia. *Biotropica*, *39*(2), 161-170.

Kuppen, E. (2017). *A hydrological analysis of the Spanish Lagoon Catchment with the AGWA model on Aruba* (Unpublished Master's thesis). Wageningen University, Wageningen, the Netherlands.

Lovelock, C. E., & Ellison, J. C. (2007). Vulnerability of mangroves and tidal wetlands of the Great Barrier Reef to climate change.

MacLean, C. D., Cole, T. G., Whitesell, C. D., Falanruw, M. V., & Ambacher, A. H. (1986). Vegetation survey of Pohnpei, Federated States of Micronesia.*Resource bulletin PSW-US Department of Agriculture, Forest Service, Pacific Southwest Forest and Range Experiment Station (USA)*.

McKay, M. D., Beckman, R. J., & Conover, W. J. (1979). Comparison of three methods for selecting values of input variables in the analysis of output from a computer code. *Technometrics*, *21*(2), 239-245.

McKee, K. L., Cahoon, D. R., & Feller, I. C. (2007). Caribbean mangroves adjust to rising sea level through biotic controls on change in soil elevation. *Global Ecology and Biogeography*, *16*(5), 545-556.

Mobile Geographics, 2017. Online Tides and Currents Predictor. Willemstad, Curacao Tide Chart. Retrieved on 4 April 2017. http://tides.mobilegeographics.com/locations/7002.html

Nagelkerken, I., Blaber, S. J. M., Bouillon, S., Green, P., Haywood, M., Kirton, L. G., Meynecke, J.O., Pawlik, J., Penrose, H.M., Sasekumar, A. & Somerfield, P. J. (2008). The habitat function of mangroves for terrestrial and marine fauna: a review. *Aquatic Botany*, *89*(2), 155-185.

Oberdorfer, J. A., & Buddemeier, R. W. (1986). Coral-reef hydrology: field studies of water movement within a barrier reef. *Coral Reefs*, *5*(1), 7-12.

Parida, A. K., & Jha, B. (2010). Salt tolerance mechanisms in mangroves: a review. *Trees*, *24*(2), 199-217.

Ramsar, 2016a. Ramsar Convention and its mission. *The Wise Use of wetlands*. Retrieved on 15 September 2016. http://www.ramsar.org/about/the-wise-use-of-wetlands

Ramsar, 2016b. Ramsar Convention Secretariat, 2010. Managing wetlands: Frameworks for managing Wetlands of International Importance and other wetland sites. Ramsar handbooks for the wise use of wetlands, 4th edition, vol. 18. Ramsar Convention Secretariat, Gland, Switzerland.

Rhoades, J. D., & Chanduvi, F. (1999). *Soil salinity assessment: Methods and interpretation of electrical conductivity measurements* (Vol. 57). Food & Agriculture Org..

Ryan, M. G., Binkley, D., & Fownes, J. H. (1997). Age-related decline in forest productivity: pattern and process. *Advances in ecological research*, *27*, 213-262.
Saenger, P., & Snedaker, S. C. (1993). Pantropical trends in mangrove above-ground biomass and annual litterfall. *Oecologia*, *96*(3), 293-299.

Sobol, I. M. (1993). Sensitivity estimates for nonlinear mathematical models. *Mathematical Modelling and Computational Experiments*, *1*(4), 407-414.

Stenberg, P., Linder, S., Smolander, H., & Flower-Ellis, J. (1994). Performance of the LAI-2000 plant canopy analyzer in estimating leaf area index of some Scots pine stands. *Tree Physiology*, *14*(7-8-9), 981-995.

Twilley, R. R., & Chen, R. (1998). A water budget and hydrology model of a basin mangrove forest in Rookery Bay, Florida. *Marine and Freshwater Research*, *49*(4), 309-323.

USDA, 2017. United States Department of Agriculture. Natural Resources Conservation Service Soils. (1998). *Soil Quality Resource Concerns: Available Water* Capacity. Retrieved on 24 April 2017. https://extension.illinois.edu/soil/sq_info/awc.pdf

Van Dam, J. C., Huygen, J., Wesseling, J. G., Feddes, R. A., Kabat, P., Van Walsum, P. E. V., Groenendijk, P. & Van Diepen, C. A. (1997). Simulation of water flow, solute transport and plant growth in the soil-water-atmosphere-plant environment. *Theory of SWAP version*, *2*, 167.

Van Dam, J.C., Metselaar, K., Van der Zee, S. (2015). Manual Ecohydrology 2015. Soil Physics and Land Management Group, Wageningen University.

Van Hoorn, J. W., & Van Alphen, J. G. (1994). Salinity control. *Drainage principles and application. 16th ed. Wageningen: International Institute for Land Reclamation and Improvement*.

Van der Werf, W., Keesman, K., Burgess, P., Graves, A., Pilbeam, D., Incoll, L. D., ... & Palma, J. (2007). Yield-SAFE: A parameter-sparse, process-based dynamic model for predicting resource capture, growth, and production in agroforestry systems. *Ecological engineering*, *29*(4), 419-433.

Van Sambeek, M. H., Eggenkamp, H. G. M., & Vissers, M. J. M. (2000). The groundwater quality of Aruba, Bonaire and Curaçao: a hydrogeochemical study. *Netherlands Journal of Geosciences/Geologie en Mijnbouw*, *79*(4).

9. Annex

Figure 1 – Photograph of the head; both the road and forested are indicated.

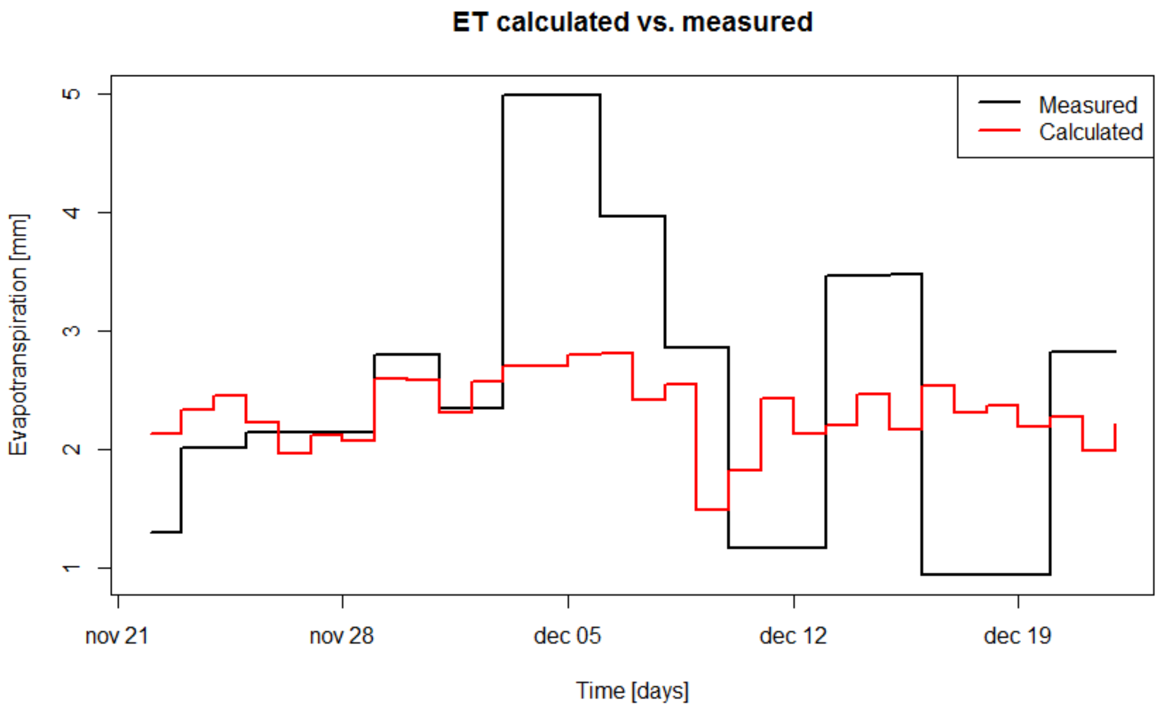

Figure 2 – Comparison of the measured ET versus the calculated ET

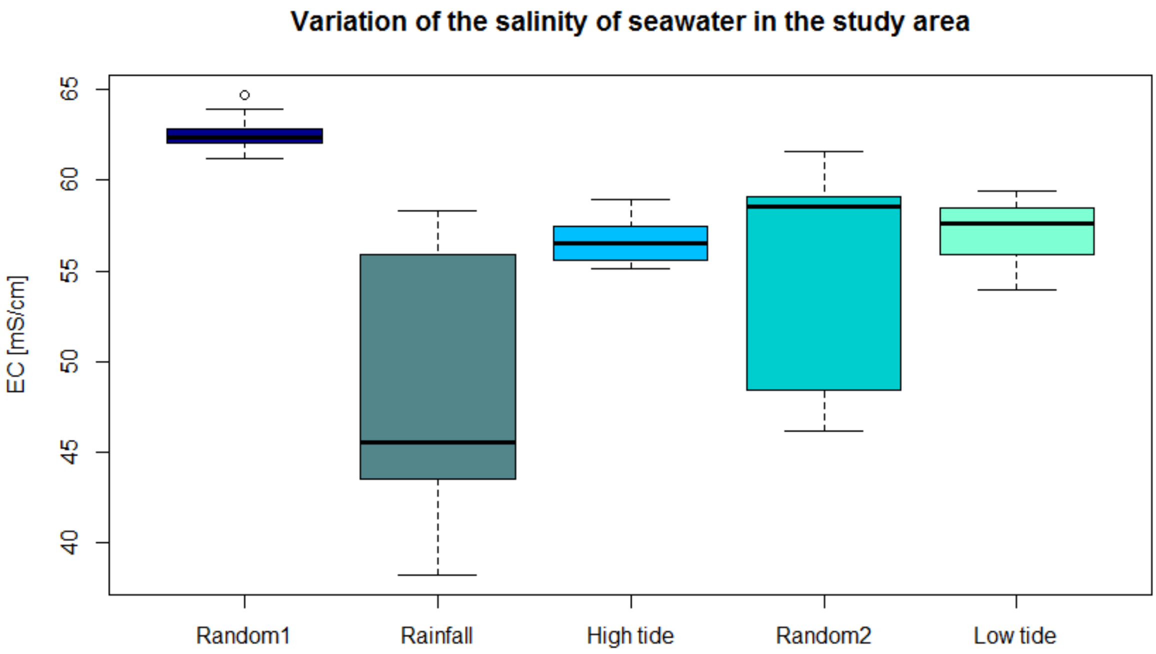

Figure 3 – Boxplot of the variation in electrical conductivity between the different measurement points. Three of the 5 measurements show little variation, however for two measurements the variation was quite large; especially after a rainfall event.

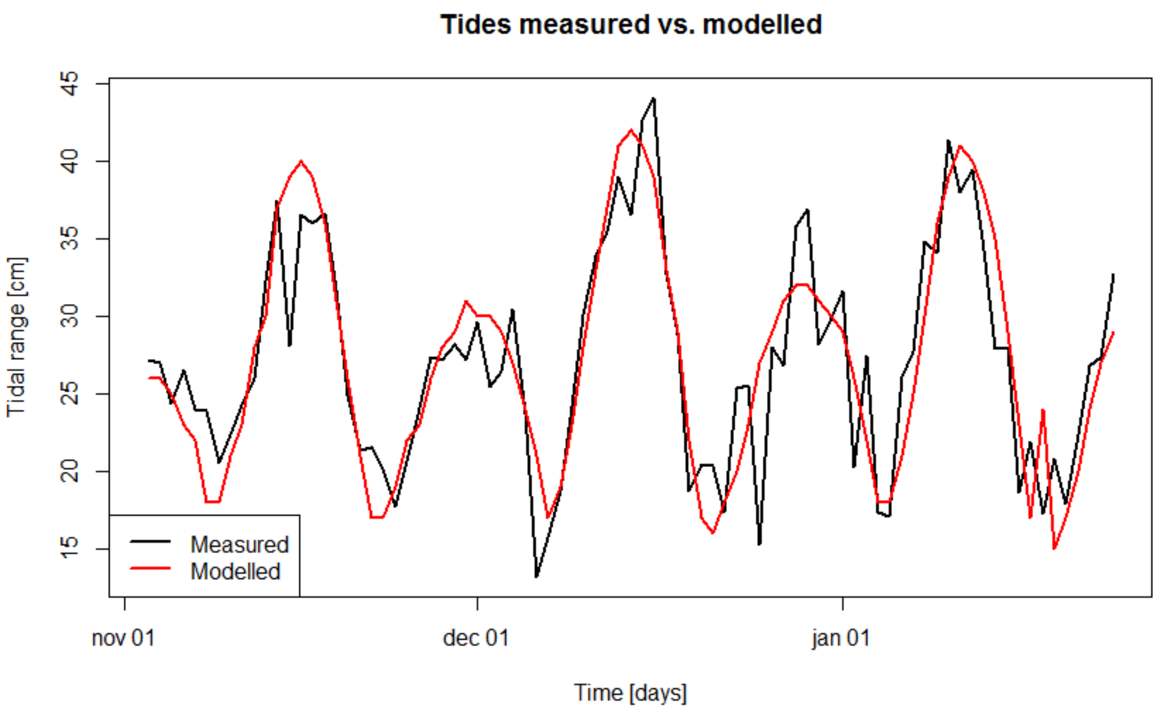

Figure 4 – Validation of the modelled tides

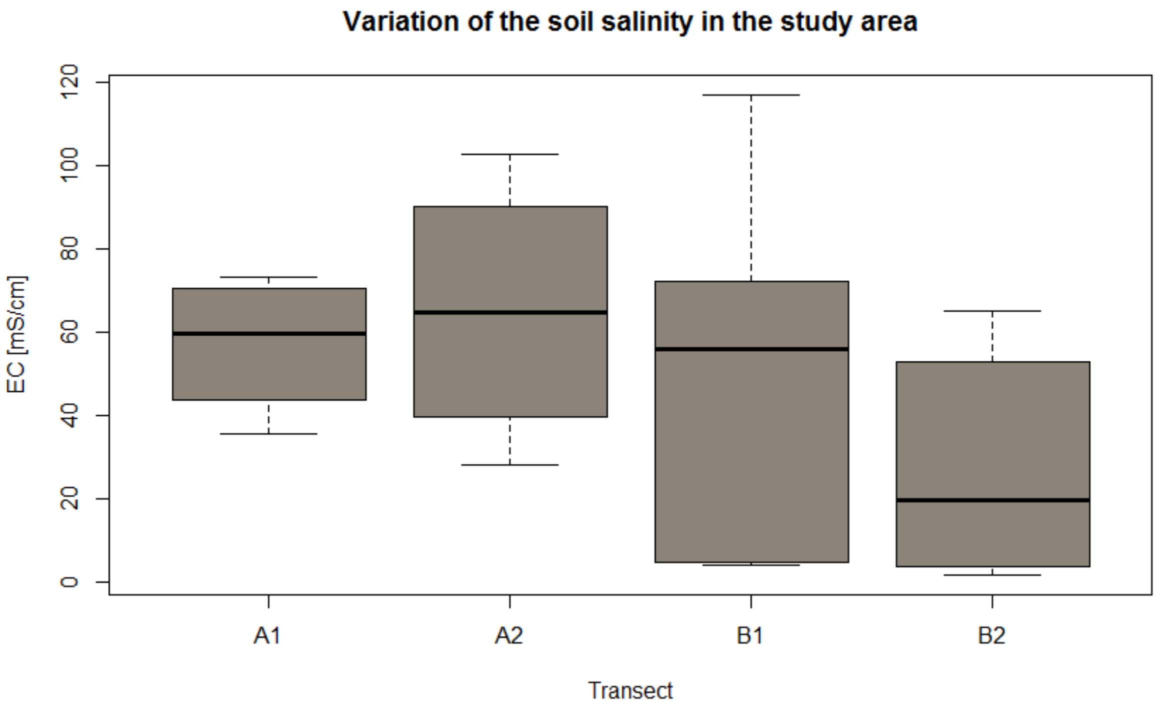

Figure 5 – Boxplot of the variation in soil salinity based on the results of the saturated paste method. In this figure “A” refers to the transect along the head and “B” to the transect along the tail. The soil salinity was determined twice.